

*Mini review*

**Atomistic modeling and molecular dynamic simulation of polymer nanocomposites for thermal and mechanical property characterization:  
A review**

**Nilesh Shahapure<sup>1</sup>, Dattaji Shinde<sup>1,\*</sup> and Ajit Kelkar<sup>2</sup>**

<sup>1</sup> Production Engineering Department, V.J.T.I., Mumbai, Maharashtra, India

<sup>2</sup> Mechanical Engineering Department, North Carolina A&T State University, Greensboro, NC, USA

\* **Correspondence:** Email: dkshinde@pe.vjti.ac.in; Tel: +91-22-24198239;  
Fax: +91-22-24198239.

**Abstract:** Epoxy resins are formed when epoxy monomers react with crosslinkers that have active hydrogen sites on them such as amine and anhydrides. These cross-linked structures are highly unpredictable and depend on different parameters during curing. Epoxy material when reinforced with nanoparticles has got importance because of its extraordinary enhanced mechanical and thermal properties for structural application. Experimentally it is challenging to tailor these nanostructures and manufacture epoxy-based nanocomposites with desired properties. An experimental approach to preparing these is tedious and costly. The improvement of such materials requires huge experimentation and a better level of control of their properties can't be accomplished up till now. There is a need for numerical experimentation to guide these experimental procedures. With the headway of computational techniques, an alternative for these experiments had given an effective method to characterize these nanocomposites and study their reaction kinetics. Molecular dynamics (MD) simulation is one such technique that works on density function theory and Newton's second law to characterize these materials with different permutations and combinations during their curing. This review is carried out for MD simulation studies done to date on different epoxies and epoxy-based nanocomposites for their thermal, mechanical, and thermo-mechanical characterization.

**Keywords:** nanocomposites; molecular dynamics; epoxy; carbon nanotubes

---

## 1. Introduction

Epoxy are thermoset resins is a synthetic polymeric material where more than one similar or dissimilar epoxy groups react with a different crosslinker to create a complex cross-linked structure. The curing of these epoxies can happen in more than one stage. This allows reinforcement to impregnate with the epoxy in the partially cured state. Generally, this curing process starts with the formation of linear low molecular weight polymers. During curing, the active groups on the crosslinker or curing agent react with the hydroxyl group of epoxide, leading to the formation of complex cross-linked network structures. This resultant cross-linked epoxy system shows a series of excellent mechanical and thermal properties such as high Young's modulus, fracture strength, high creep resistance, and high-temperature performance. A polymeric nanocomposite is a group of composites that have one of the reinforcement phases at a nanometric scale. With these reinforcement thermal and mechanical properties of composite material improves dramatically. Hence, many experimental and theoretical studies were carried out to explore the potential application of these epoxy reinforced with different scales of reinforcement. Since the experimental techniques to characterize these materials is a costly and tedious process so there is a need for computational techniques to carry out this process which gives better insight into the different aspects during the fabrication of these nanocomposites. Molecular dynamic simulation is one such technique that works on Newton's second law and DFT gives an idea about what happens at the molecular level because of which how mechanical and thermal properties at the microscopic level are going to vary.

## 2. Characterization techniques

The characterization techniques for polymeric nanocomposites adopted by different researchers in the last few decades were experimental, classical, and quantum mechanics-based approaches. Each of these characterizing procedures has certain benefits and challenges related to them. Experimental techniques are time-consuming and costly due to which most researcher relies on computational technique for understanding the difficulties during tailoring the properties of nanocomposites [1]. Some of the experimental techniques which were used are spectroscopy techniques like FTIR and X-ray scattering which are useful for the determination of material constituents, and purity of the materials, to find the impurities in the material [2]. An atomic force microscope can be used to investigate structural morphology at a nanometer scale [3]. Transmission electron microscopy can be used to understand the mechanics, fracture, and failure processes of the interface between nanomaterial and polymer matrix [4]. For different thermal and thermos-mechanical characterization, differential scanning calorimetry (DSC), thermogravimetric analysis (TGA), Fourier transformed infrared spectroscopy (FTIR), thermomechanical analysis (TMA), dynamic mechanical analysis (DMA) was used by different researcher to analyze how thermal analysis methods can help to explain the effect of addition of nanofiller in polymeric nanocomposites on its mechanical and thermos-mechanical properties. There is an effect on thermal properties such as glass transition temperature, coefficient of thermal expansion, heating effect, and rate of heating on cure kinetics [5]. There are multiple reasons why experimental studies in the range of nanometric scale are tedious and time-consuming. Out of these some of them are, the effect of the size of the specimen used for the investigation, precision lag in indirect measurement used to measure the output parameter, very few

direct measurement techniques at nanometer-scale, no redundant techniques for preparation of the specimen for nanometric observation and lack of control over the even dispersion of nanomaterial in the matrix. Computational techniques utilized for the characterization of polymeric nanocomposites is a very broad area that has different lengths and time scales to study numerous different aspects of polymer nanocomposites.

### 3. Computational techniques used for material characterization

Computational techniques utilized so far can be generally divided into three types on the basis of time and length scale as shown in Figure 1a, Molecular scale, Mesoscale, and macroscale methods. Techniques at the molecular scale are molecular dynamics (MD), Monte Carlo simulation, Microscale methods such as Brownian dynamics, dissipative particle dynamics (DPD), dynamic density functional theory (DFT) method, mesoscale and macroscale methods (e.g., micromechanics, equivalent-continuum, and self-similar approaches, finite element method (FEM) [6,7].

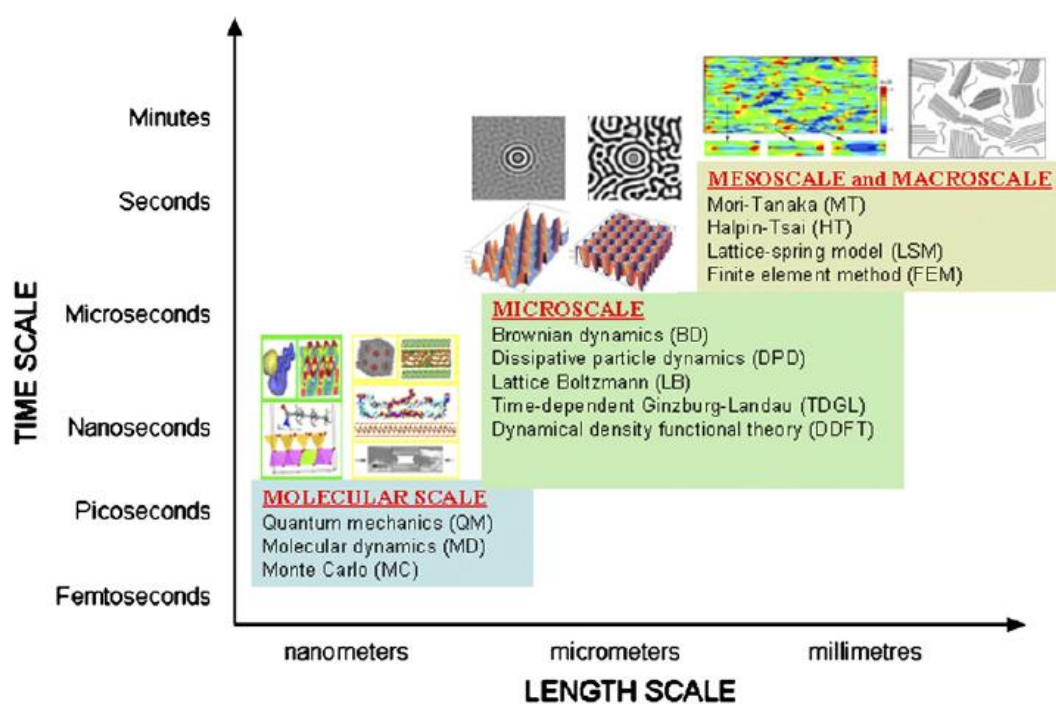
#### 3.1. Molecular scale methods

Atoms, molecules and group of molecules will be considered as basic unit in molecular level modeling and simulation. Main issues addressed in the modeling and simulation of polymer nanocomposites at molecular level are cure kinetics, rheology, final molecular structure and their interaction. Most popular methods adopted are Molecular dynamics, Monte Carlo, quantum mechanics.

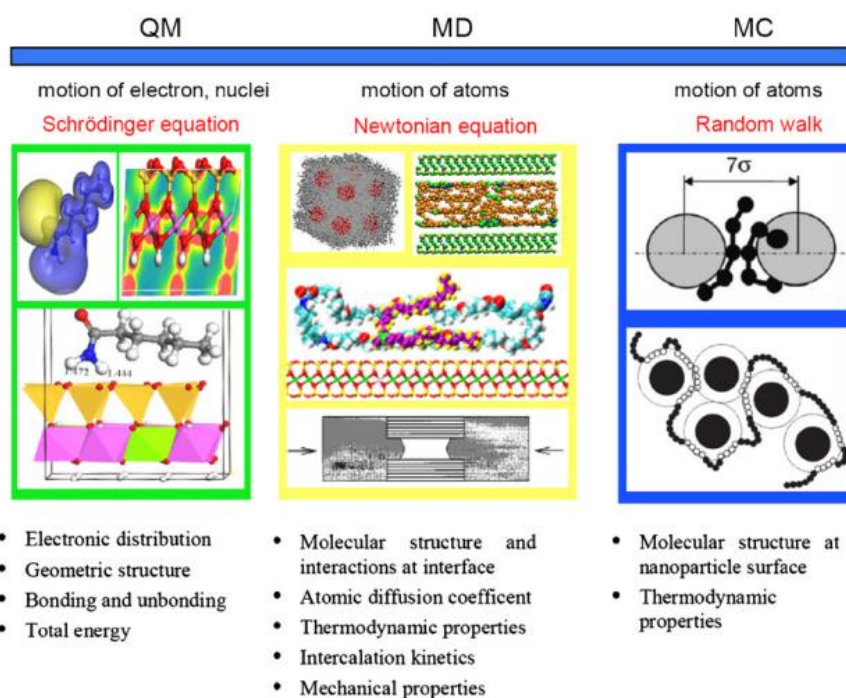
The diagram in Figure 1b describes the equation of motion for each method and the typical properties predicted from each of them [8–13].

MD simulation is used to estimate the different mechanical and thermal properties of polymer nanocomposites predicted from the interaction of atoms, molecules, or groups of molecules with respect to time under different thermodynamic states. Information on atomic positions, velocities, and forces generated from it is used to derive different macroscopic properties (e.g., pressure, energy, heat capacities) by using statistical mechanics [14,15].

The MC technique, also known as the Metropolis method, in which a sample of the population is generated using random numbers. The steps involved in MC simulation are as follows: (i) Convert the studied physics problem into a statistical or probabilistic model. (ii) Resolution of the probability model by numerical sampling method. (iii) Analyze the obtained data by statistical methods. This technique is only for balanced properties, while MD is for unbalanced as well as balanced properties [16].



(a)



(b)

**Figure 1.** (a) Time and length scale approaches for multiscale modeling and simulation (Reprinted from Ref. [6] with permission), (b) Molecular modeling and simulation methods commonly used for polymer nanocomposites (Reprinted from Ref. [6] with permission) [8–13].

### 3.1.1. Microscale methods

Specifically, in nanoparticle-polymer systems, the study of structural evolution (i.e., dynamics of phase separation) involves the description of bulk flow (i.e., hydrodynamic behavior) and the interactions between nanoparticle and polymer components. Therefore, various simulation methods have been evaluated and extended to study the microscopic structure and phase separation of these polymer nanocomposites, including BD, DPD, LB, time-dependent Ginzburg–Landau (TDGL) theory, and dynamic DFT. In these methods, a polymer system is usually treated with a field description or microscopic particles that incorporate molecular details implicitly hence, they are able to simulate the phenomena on length and time scales that are not addressable by the classical MD methods [6].

### 3.1.2. Brownian dynamics

Brownian dynamics simulation works similarly to MD simulations only some new approximations allow one to perform simulations on the microsecond timescale which is not possible in MD simulation. In BD the explicit description of solvent molecules used in MD is replaced by an implicit continuum solvent description and hence the internal motions of molecules are ignored, allowing a much larger time step than that of MD [6]. Therefore, BD is particularly useful for systems where there is a large gap in the time scale governing the motion of different components. However, if the detailed motion of the solvent molecules is concerned, they may be removed from the simulation and their effects on the polymer are represented by dissipative random force terms. Thus, the forces in the governing are replaced by a Langevin Eq 1,

$$F_t = \sum_{j \neq i} F_{ij}^C - \gamma p_i + \sigma \zeta_i(t) \quad (1)$$

where  $F_{ij}^C$  is the conservative force of particle  $j$  acting on particle  $i$ ,  $\gamma$  and  $\sigma$  are constants depending on the system,  $p_i$  the momentum of particle  $i$ , and  $\zeta(t)$  a Gaussian random noise term.

### 3.1.3. Dissipative particle dynamics

Both Newtonian and non-Newtonian fluids, including polymer melts and blends, can be simulated on the microscopic length and time scales. A DPD particle is defined by mass  $M_i$ , position  $r_i$ , and momentum  $p_i$ . The interaction force between two DPD particles  $i$  and  $j$  can be expressed as  $F_i(t)$ , the sum of conservative  $F_{ij}^C$ , dissipative  $F_{ij}^D$ , and random force  $F_{ij}^R$  as shown in Eq 2. Forces occur in pairs and momentum is conserved, so the macroscopic behavior is directly related to Navier-Stokes hydrodynamics. However, the energy is not conserved due to the presence of dissipation and random force terms similar to BD, but including the effect of Brownian motion on larger length scales [17–19].

$$F_i(t) = \sum_{j \neq i} F_{ij}^C + \sum_{j \neq i} F_{ij}^D + \sum_{j \neq i} F_{ij}^R \quad (2)$$

### 3.1.4. Lattice Boltzmann

The LB method derives from the lattice gas automaton constructed as a fictional, simplified molecular dynamics where space, time, and particle velocities are all discrete [20]. The main feature of the LB method is to replace the displacement variables of the particle with single-particle distribution functions and ignore the individual particle motion and particle-particle correlation. An important advantage of the LB method is that the microphysical interactions of liquid particles can be easily included in the numerical model. Compared with the Navier-Stokes equations, the LB method can handle interactions between fluid particles and reproduce the micro-scale mechanism of hydrodynamic behavior.

### 3.1.5. Time-dependent Ginzburg-Landau method

This technique is used for the simulation of structural evolution of phase separation in polymers and block copolymers. In this method, temperature reduction from the miscible to immiscible region of the phase diagram is simulated by minimizing the free energy function. Glotzer has applied this method to polymer blends and particle filled polymer systems [21].

### 3.1.6. Dynamic DFT (Density Functional Theory) method

Dynamic DFT method has been implemented in the software package Mesodyn TM from Accelrys and models polymers dynamic behavior by combining TDGL model with statistics of Gaussian mean field for time advancement of parameters [22]. A similar DFT methodology was adopted by authors [23,24] and created the basis for their new software tool Simulation Interfaces (SUSHI) which can address soft and hard interfaces, one of a suite of molecular and mesoscale modeling tools (called OCTA) developed for the simulation of polymer materials [25].

### 3.1.6. Mesoscale and macroscale methods

Despite the importance of understanding the physical properties and molecular structure, their behavior can be normalized at different scales for different aspects. Macroscopic behavior is often explained without considering discrete atomic and molecular structures, and it is also based on the assumption of a continuous distribution of the material throughout its volume, resulting in an average density. Continuity models based on these laws must be combined with appropriate constitutive equations. Therefore, the properties of the local continuity are statistically represented by developing representative volumetric elements (RVE) in micromechanical models. Micromechanical engineering can represent interfaces between discontinuities, components, and combined mechanical and non-mechanical properties.

## 4. Atomistic modeling and molecular dynamics

Computer modeling and simulation will be the most emerging field in the prediction of molecular-level behavior for polymer nanocomposites. Computer modeling of the constituent's materials and simulation are specially used to address the following fundamental concerns:

- (1) The reaction kinetics and its dependence on temperature changes during the formation of polymer nanocomposites.
- (2) Structure and its properties associated with it and its dynamics for polymer nanocomposites ranging from the molecular scale to macro scale.
- (3) Behavior of polymer on the addition of nanoparticles and its rheological changes, to optimize the process parameters during the manufacturing of composite material.
- (4) The reinforcement mechanisms of nanoparticles in the polymer [26].

MD is a semi-empirical formulation of a system, to study the movement of atoms and molecules under different thermodynamic states. Thermodynamic states or ensembles are the essential requirements to carry out the MD simulations. The ensemble is an arrangement of all the diverse microstates of a framework that can exist in a system of molecules under consideration. Different macroscopic constraints lead to different ensembles. The micro-canonical, canonical, isobaric-isothermal, and isenthalpic were the most widely used ensembles [27].

To carry out an MD simulation of any material, a simulation box of equal side length was considered. This box contains  $N$  atoms of the given material. The initial position and velocity of all these atoms were considered as  $x(a)$  and  $\dot{x}(a)$  respectively. The energy between atoms was defined by a specific form of interatomic potential. The Interatomic potential was the energy stored in the bonds when it was subjected to some external force which is analogous to strain energy in classical mechanics. The main objective of MD simulation is to determine the positions  $r_a(t)$ , and momenta  $p_a(t)$ , of these  $N$  atoms over time period “ $t$ ”. From these positions, displacement and strain can be extracted. The atoms are assumed to behave classically and hence obey Newton’s second law of motion defined as in Eq 3,

$$m_a \frac{d^2 r_a}{dt^2} = F_a; \quad a = 1, \dots, N \quad (3)$$

Where  $m_a$  is the mass of the particle “ $a$ ” and  $F_a$  is the force acting on the “ $a$ ”th particle. The appropriate numerical integration can be used to all such scalar equations to get final values of all the energy terms as addressed by Sindu & Sasmal [28].

While performing any such physical simulation proper interatomic potentials, appropriate selection of numerical integration method adopted for convergence, periodic boundary conditions applied to mimic the physically meaningful system, and the controls of pressure and temperature will be done through proper selection of thermodynamic ensembles. The interaction potentials and their parameters will describe how the particles in a system interact with each other particles in the system, i.e., how the potential energy of a system depends on the particle coordinates. These force fields or interaction potentials may be obtained by a quantum method like ab-initio, empirical methods like Lennard–Jones, Mores, Born-Mayer, and quantum-empirical methods like embedded atom model, and bond order potential. The right choice of force field will lead to accuracy, transferability, and an increase in computational speed [29].

General terms in any interaction potential  $U$  typically consists of bonded, and nonbonded interaction respectively as shown in Eq 4 [30]. Different interaction potential terms associated with graphene structure were shown in Figure 2. The bonded interaction terms were  $U_{\text{bond}}$ , i.e., energy term associated with stretching of bond,  $U_{\text{angle}}$  was energy term associated with the bending of bonds and dihedral angle torsion is the term associated with twisting of the bond during interaction i.e.  $U_{\text{torsion}}$  and inversion interaction  $U_{\text{inversion}}$ . The last two terms are non-bonded interactions, i.e., van

der Waals energy  $U_{vdw}$  and electrostatic energy  $U_{electrostatic}$ . In Eq 4,  $\vec{r}_a, \vec{r}_b, \vec{r}_c$ , and  $\vec{r}_d$  are the positions of the atoms in typical graphene structure involved in a given interaction;  $N_{bond}$ ,  $N_{angle}$ ,  $N_{torsion}$  and  $N_{inversion}$  are the number of atoms involved in these respective interactions in the simulated system. Whereas  $i_{bond}$ ,  $i_{angle}$ ,  $i_{torsion}$ , and  $i_{inversion}$  uniquely specify an individual interaction of each type;  $i$  and  $j$  in the van der Waals and electrostatic terms indicate the atoms involved in nonbonded interaction.

$$\begin{aligned}
 & (\vec{r}_1, \vec{r}_2, \dots, \vec{r}_N) \\
 = & \sum_{i_{bond}}^{N_{bond}} U_{bond}(i_{bond}, \vec{r}_a, \vec{r}_b) + \sum_{i_{angle}}^{N_{angle}} U_{angle}(i_{angle}, \vec{r}_a, \vec{r}_b, \vec{r}_c) \\
 & + \sum_{i_{torsion}}^{N_{torsion}} U_{torsion}(i_{torsion}, \vec{r}_a, \vec{r}_b, \vec{r}_c, \vec{r}_d) \\
 & + \sum_{i_{inversion}}^{N_{inversion}} U_{inversion}(i_{inversion}, \vec{r}_a, \vec{r}_b, \vec{r}_c, \vec{r}_d) + \sum_{i=1}^{N-1} \sum_{j>i}^N U_{vdw}(i, j, \vec{r}_a, \vec{r}_b) \\
 & + \sum_{i=1}^{N-1} \sum_{j>i}^N U_{electrostatic}(i, j, \vec{r}_a, \vec{r}_b)
 \end{aligned} \tag{4}$$

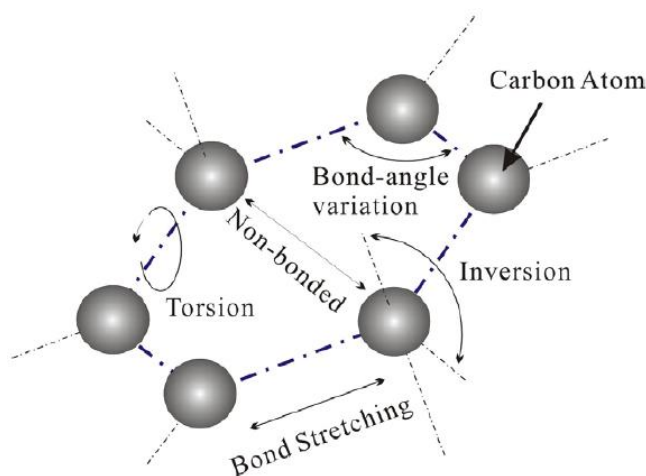


**Figure 2.** Typical Bond structures and energy terms associated with respective interaction in a graphene cell (Reprinted from Ref. [30] with permission).

Commonly used force fields in MD simulation of epoxy/CNT nanocomposites were COMPASS, PCFF, MM3, ReaxFF, UFF, Dreiding, OPLS, and MMFF [31–35]. Some of these were generalized force fields like dreiding and some were very suitable for large size organic molecules such as ReaxFF, COMPASS.



## 5. Molecular dynamics techniques for mechanical characterization of polymeric nanocomposites

Among the different types of thermosets, epoxy is known for its compatibility with current lightweight structures for aviation and automobile applications [1]. It has been seen that the properties of epoxy improved with CNT, and graphene reinforcement [7,36]. Findings in the literature show that using nanofillers and conventional microscale fibers together, as multiscale reinforcement improves composites' mechanical properties, which are impossible in conventional composites. As is notable, damage inception increases with the increase in applied load, and a small crack at the interface between the fiber-matrix may decrease the fatigue life of composites. With the insertion of nanofillers toughening of the interfacial fiber-matrix region will happen. Hence, we can increase the threshold value of damage initiation which can lead to the fabrication of reliable composite materials for different applications [37].

Molecular Dynamics studies were carried out to investigate the interaction of Carbon Nanotube (CNT) with different morphologies and different types of epoxy polymers [28]. Most Commonly used resins and hardeners in the industries were used for the study. Steered Molecular Dynamics simulation of epoxies and CNT with different combinations of chirality, and diameters of CNTs were carried out. Pull-out simulations under constant pulling velocity conditions were carried out and their results were studied. An interaction study of epoxy-CNTs was done and a new parameter called affinity index was proposed in the present study to quantify the interaction of the polymer with CNT. The variation of affinity index with time step will be helpful for the right selection of resin and hardener combination for selected morphology of CNTs. To verify the results of the affinity test number of Pull-out simulations were carried out. They found that pull-out test results were in good agreement with the affinity test.

Molecular dynamics simulation was performed for the mechanical properties characterization of polycarbonate reinforced with single-walled armchair carbon nanotubes [36]. Estimation of young's modulus, shear and bulk moduli, and Poisson's ratio was done by constant-strain methodology in MD simulation of PC/CNT nanocomposites. In this simulation effects of different parameters like weight fraction and aspect ratio of CNTs on the elastic properties of nanocomposites were studied. The results of the simulation show that the elastic moduli of PC/CNT nanocomposites increased as there was an increase in the amount of CNTs. The aspect ratio ( $l/d$ ) of CNTs also shows the same trend that elastic properties increase with the increase in aspect ratio.

Zaminpayma did the molecular dynamics simulation to study the interaction between polythiophene, polyethylene, poly(p-phenylenevinylene) abbreviated as PT, PP, and PPV respectively, and CNTs by using reactive force field (ReaxFF) which reveals the formation and breaking of bonds during the curing process [37]. Other nonreactive force fields like COMPASS will form the bonds on the basis of cut-off distance hence there was no assurance that the correct system was built or not for mechanical characterization. The effect of CNT diameter, types of polymer, and temperature on interaction energy was studied. Larger CNT at low temperatures shows stronger interaction energy with polythiophene. Mechanical properties such as the breaking stress and strain, and Young's modulus had a direct relation with interaction energy. CNTs-polymer composites interaction energy increases with an increase in the diameter of CNT and decreases with a decrease in temperature. They found that interaction between PT-CNT and PPV-CNT was stronger than PP-CNT as shown in Figure 3a,b due to the presence of aromatic rings in their structures.

Arash Wang found that Young's modulus and yield strength of the interfacial region is considerably influenced by interfacial interactions between carbon nanotubes and polymer matrix in CNT/PMMA composites [38]. They developed a new method using MD which was based on the fracture behavior under the tension of carbon nanotube reinforced poly(methyl methacrylate) (PMMA) matrix composites for evaluation of the elastic properties. The aspect ratio of CNT affects the interfacial strength significantly as CNT with infinite length was subjected to pull-out simulation. The result of this simulation reveals that Young's modulus value increased dramatically and hence it can be concluded that the resultant nanocomposite was stiffer than the PMMA matrix. For the prediction of elastic properties of the nanocomposites a three-phase micromechanical model having fiber, matrix, and interphase as three phases also developed since two-phase models like the Mori–Tanaka method suitable for fiber of length in microns or more than that which are not suitable for short fibers.

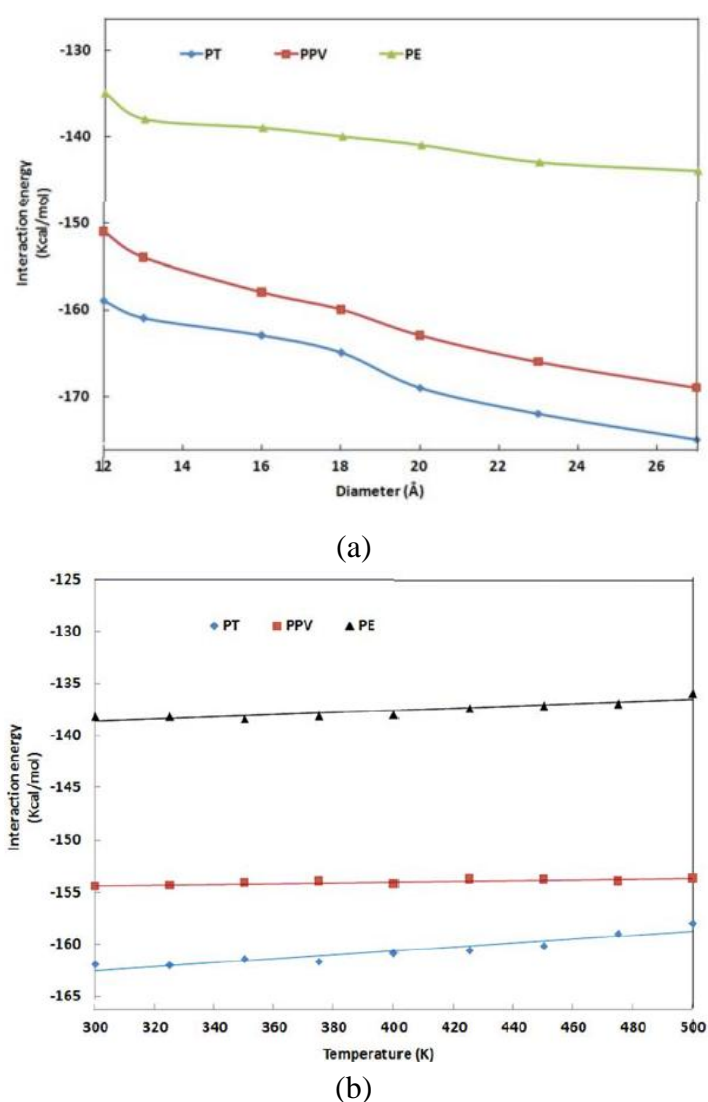


**Figure 3.** (a) Interaction energy between a CNT-polymer as a function of CNT diameter at 300 K, (b) Variation of the Interaction energy between CNT-polymer as a function of temperature for (10,10) CNT (Reprinted from Ref. [37] with permission).

A study was done on Molecular dynamics simulation to compare the simulation output by different force fields for the verification of physical and mechanical properties [39]. Diglycidyl ether of bisphenol-A and diethylene triamine (DETA) as resin, hardener combination was used and a constant-strain (static) approach was adopted. The result of simulation by using COMPASS, PCFF, UFF, and Dreiding force fields with the same initial structure when compared with experimental results showed that COMPASS and PCFF results were more reliable for polymeric materials.

In the Molecular dynamics (MD) simulations of the same resin with different hardeners combination study done for the thermal and mechanical characterization reveals that DGEBA resin has better properties with DETDA compared to TETA hardener [40]. Simulation studies were carried out for the thermal and mechanical properties of DGEBA/TETA and DGEBA/DETD. They observed that at lower cross-linking density the value of glass transition temperature was better in agreement with the experimental result for DGEBA/DETD this was attributed to the size of the simulation cell and the number of molecules under consideration during this simulation. They observed that the mechanical properties of DGEBA/TETA were more than DGEBA/DETD for all cross-linking densities.

Shenogina et al. carried out the molecular dynamics simulations to study thermo-mechanical properties of cross-linked polymers made of DGEBA and DETDA with different degrees of crosslinking [41]. The approach adopted by them for crosslinking allowed them to produce high degrees of conversion with stress-free molecular models. They tried to find the effect of model size under consideration and observed that at smaller volume, glass transition temperature value will be more attributed it to less possibilities for structural rearrangements. The coefficient of thermal expansion will be increasing with the increase in volume of model size and density will be less since more time required for equilibration. The length of epoxy strands shows better conversion for coefficient of thermal expansion, density with experimental values for longer chain length of monomers/dimers/trimers unit cells. For Infinite length chains no result was observed. The structures with oligomers show the better agreement with experimental values. The computationally efficient static deformation approach was adopted for the calculation of thermos-mechanical properties. Averaging of these properties was done to predict the macroscopic properties of the sample. This approach allows a macroscopically homogeneous amorphous material can be viewed as heterogeneous at the nanoscale.

A multiscale model of polymer nanocomposite was created by Choi et al. [42]. MD simulation followed by three-dimensional FE analysis was adopted to characterize the interface between SiC nanoparticles and epoxy polymer. Interface identification is done on the basis of the procedure adopted as shown in Figure 4 by using the continuum model. Energy density due to deformation obtained from MD simulation inverse homogenization procedure was used to predict the effective modulus of the interface which governs the properties of the nanocomposite. From these properties of the interface, the thickness of the interface and continuum phase was calculated. In the later part of the study, they addressed the effect of nanoparticle size on the overall mechanical property variation of composites. The thickness of the interface which governs the effective properties of the composite increases with the increase in particle radius due to non-bond pairs between the reinforcement and matrix constituent atoms. As particle size decreases mechanical properties of the interface improved. The effect due to curvature of the particle can be neglected as particle size increases above 10 nm.

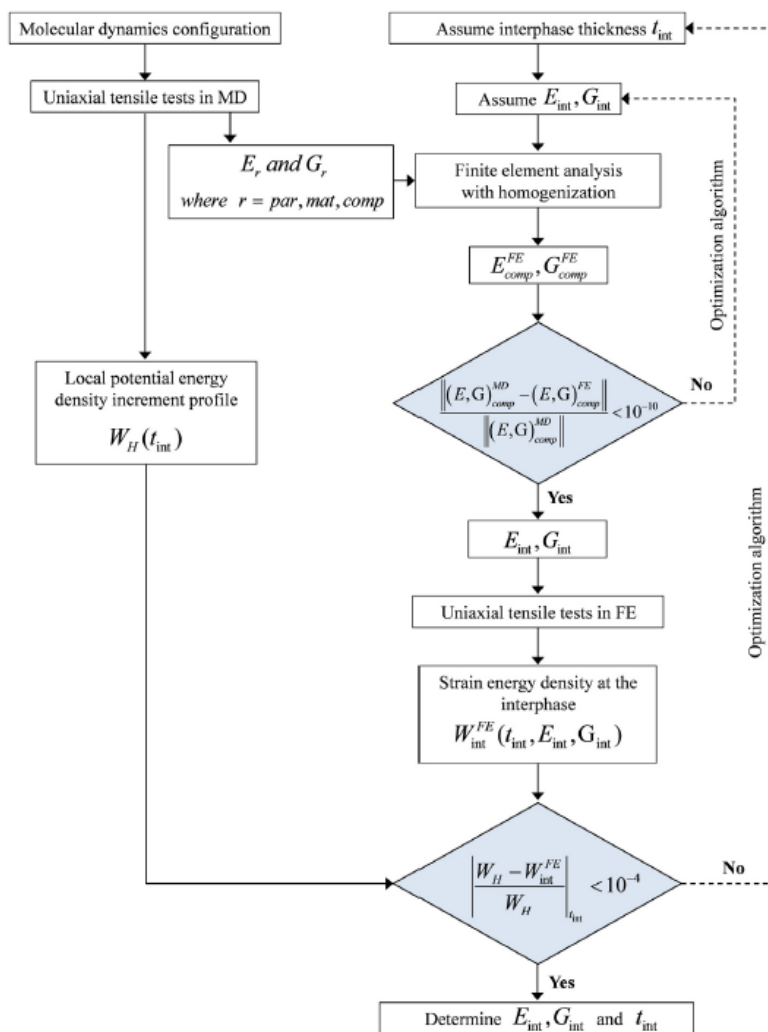


**Figure 4.** Multiscale approaches for the prediction of interfacial geometry and mechanical properties (Reprinted from Ref. [42] with permission).

Ingvason and Rollin used MD simulation to carry out pull-out simulation of SWCNT in DGEBF epoxy and DETDA hardener resin system. They observed the tensile strength of SWCNT by MD simulation to be around 1.4 TPa at 300 K [43].

Volodin et al. modeled coiled CNT in MD simulation show significant improvement in the properties of nanocomposite than straight CNT [44]. The straight-type nanotubes and the matrix have weak bonding hence coiled nanotubes were the better choice. Mechanical interlocking properties of coiled CNT increase the shear stiffness of nanocomposites due to the spring link structure of these CNTs. For the Improvement of the mechanical properties of CNT/epoxy nanocomposite, interfacial properties were the most important criterion. Functionalization of carbon nanotubes was one most suitable ways that improve the dispersion of carbon nanotubes in a matrix material which leads to modifying the characteristics of the interface and results in improved mechanical properties of polymer nanocomposites [45].

An MD simulation on DGEBF and DETDA with SWCNT with vacancy defects in it for mechanical characterization was done by Mohan et al. [46]. The vacancy defects in the SWCNT structure were intentionally introduced by removing carbon atoms from any one side of the carbon

nanotube as shown in Figure 5a–e. By the introduction of vacancy defects, they observed that Young's modulus of the material goes on decreasing as the number of defects was increasing. This shows that carbon vacancy defects are one of the potential causes that lower Young's modulus values of Epoxy-SWCNT composite as shown in Figure 6.

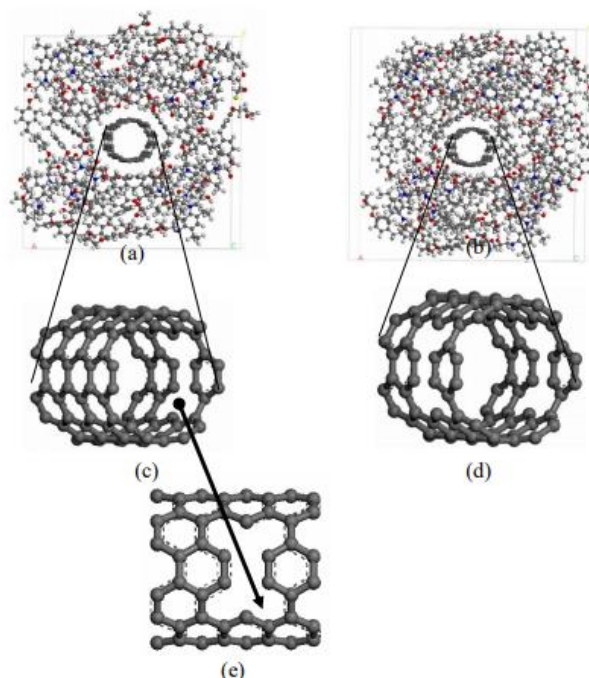


**Figure 5.** (a) Simulation cell reinforced with 2 defect CNT, (b) Simulation cell reinforced with 4 defects CNT, (c) Zoomed view of 2 defects in CNT, (d) Zoomed view of 4 defects CNT, (e) Side view of defective CNT (Reprinted from Ref. [46] with permission).

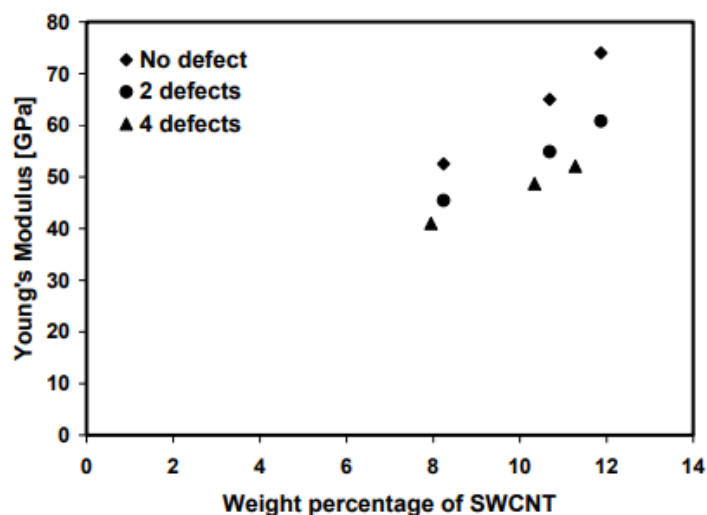


**Figure 6.** Variation of Young's modulus with SWCNT wt% with different amounts of defects in CNT (Reprinted from Ref. [46] with permission).

Rahman et al. carried out an MD simulation of CNT/epoxy nanocomposite and used this data in machine learning to predict the critical value of pull-out force in the interfacial region of the epoxy-CNT interface [47]. Radial distribution function was used to extract the data of the chemical environment near CNT from MD simulation and the same was assigned to train the neural network for prediction of the pull of force in the interfacial region. They observed that the prediction of the critical value of pull-out force has greater accuracy. This model can be used as an optimization scheme to maximize the shear strength of CNT-epoxy interfaces and as a guiding tool for experimental work. The model scheme adopted is shown in Figure 7.

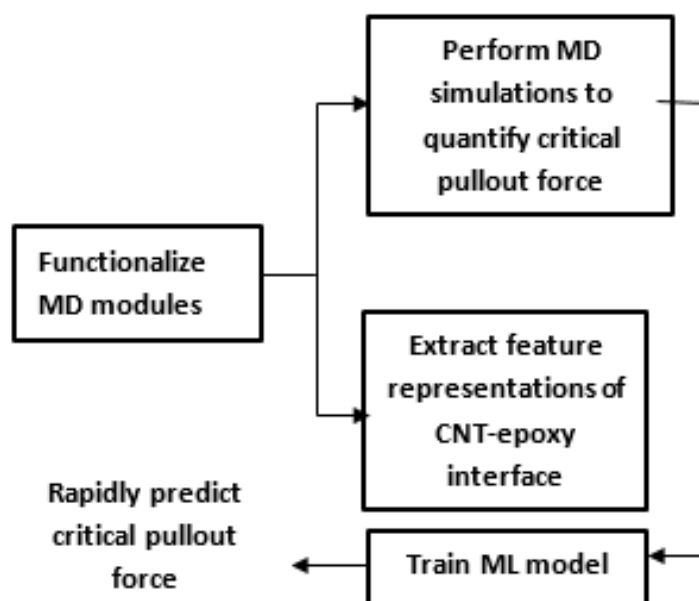


**Figure 7.** Schematic representation of the overall modeling framework (Reprinted from Ref. [47] with permission).

A Spring-bead model to represent clusters of polymer bonds at the nanoscale of epoxy to minimize the computational error during strain energy calculation which overcomes the nanoscale heterogeneous structure to microscale homogenous structure to the development of nano to microscale multiscale model as shown in Figure 8 [48]. This model can be used for the prediction of the macroscopic properties of the materials. In this spring-bead model, two beads serve as half mass of the bond cluster and it acts as a linear spring to capture the mechanical response of the bond cluster. The potential energy stored in the spring due to elongation or contraction captures the elastic strain energy in the deformed material. It was taken care that the definition of spring-bead model was dependent on the size of the bond cluster thus the right selection of the bond cluster as spring-bead computational time will be reduced and faster prediction of macroscopic properties can be achieved.

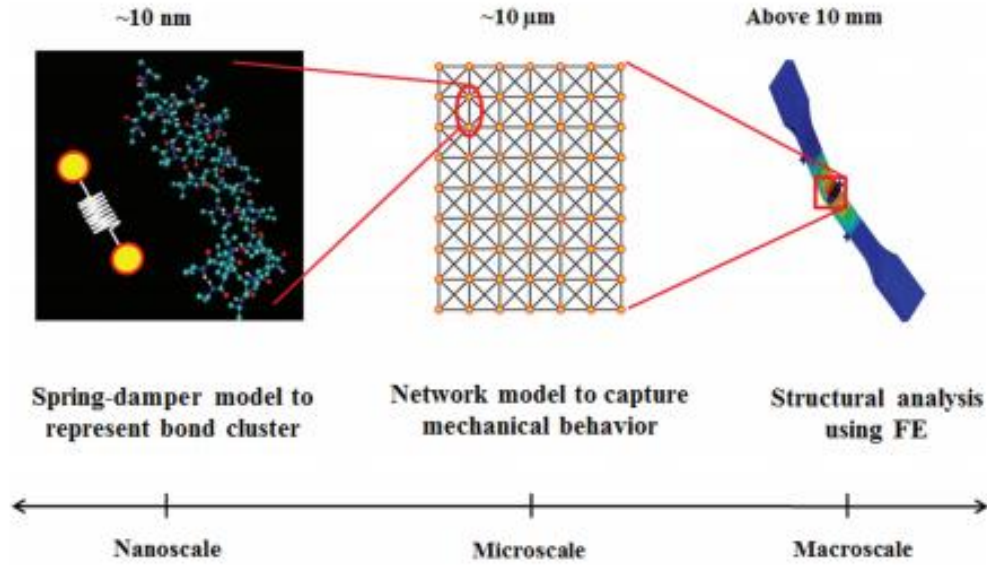


**Figure 8.** Modeling of polymer materials from the nanoscale to macroscale (Reprinted from Ref. [48] with permission).

Park & Yun used MD simulation to determine interfacial shear modulus by applying shear deformation model between epoxy and functionalized graphene [49]. They carried out MD simulation of pull-out test to characterize the interfacial properties between graphene and cured epoxy as shown in Figure 8. Here first interfacial energy was calculated by using Eq 5, and the pull-out force was estimated by using Eq 6. From this interfacial shear modulus was estimated by using Eq 7.

$$E_{int} = \text{interfacial energy} = E_{total} - (E_{matrix} + E_{graphene}) \quad (5)$$

$$F_i = \text{pullout force} = \lim_{\Delta x \rightarrow 0} \frac{\Delta E_{int}}{\Delta x} = F_i = \frac{4bG_i}{T-t} \int_{-\frac{t-x}{2}}^{\frac{t-x}{2}} (u_g - u_i) ds \quad (6)$$

Where  $G_i$  = interfacial shear modulus,  $T$  &  $t$  = thickness of the top and bottom interfacial region. where  $u_g$  and  $u_i$  are the displacements of the matrix adjacent to the graphene and outer matrix, respectively

$$G_i = \frac{\frac{T-t}{4b} F_i}{\int_{-\frac{t-x}{2}}^{\frac{t-x}{2}} (u_g - u_i) ds} \quad (7)$$

$L$  = total length of contact between graphene and epoxy on either side,  $b$  = width of graphene sheet considered.

Kallivokas, Sgouros & Theodorou studied the DGEBF, DETDA system for the topological, structural and dynamic behavior of material with respect to time and temperature by using MD simulation. They first time attempted to simulate the experimental XRD result by using MD simulation [50].

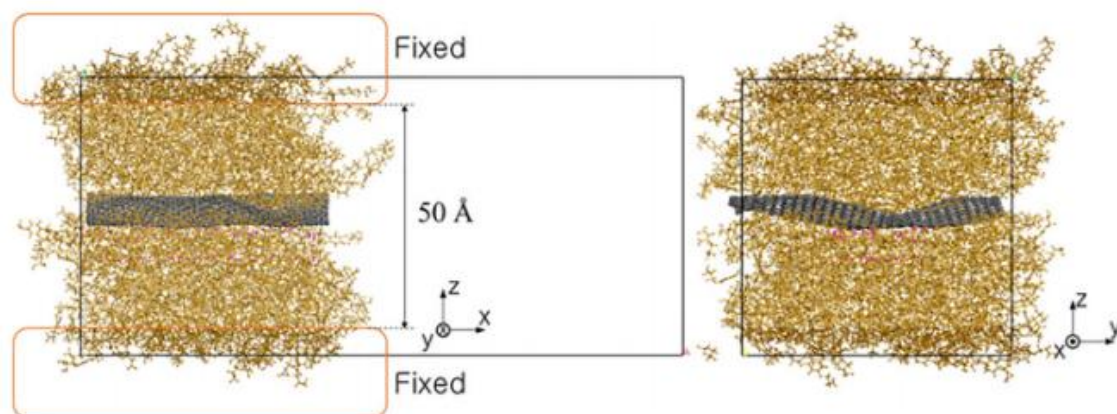


**Figure 9.** Graphene/epoxy system for pull-out simulation (Reprinted from Ref. [49] with permission).

Aghadavoudi et al. did the experimental investigation and multiscale modeling and simulation by using MD for the mechanical property evaluation of epoxy graphene nanoplatelets, and CNT hybrid nanocomposite [51]. An equivalent fiber method was used to convert the elastic constant obtained from the MD simulation to microscale values. Thus, a new multi-scale modeling approach was developed which rivals that experimentally calculated mechanical properties were in good agreement with simulation results as shown in Table 1. Where  $E_{h1}$  and  $E_{h2}$  are Young's modulus of CNT/epoxy and GNP/epoxy nanocomposites and  $E_{\text{Hybrid}}$  is equivalent to Young's modulus of hybrid nanocomposite calculated by equivalent fiber method.

**Table 1.** Comparison of predicted and experimental Young's modulus calculated by equivalent fiber method (Reprinted from Ref. [51] with permission).

Sample	Material	$E_{h1}$ (MPa)	$E_{h2}$ (MPa)	$E_{\text{Hybrid}}$ (MPa)		Diff. %
				Theoretical	Experimental	
1	GNP (0.375%) CNT (0.375%) Epoxy (99.25%)	3.33	3.06	3.20	3.128	2
2	GNP (0.25%) CNT (0.75%) Epoxy (99%)	3.87	2.98	3.43	3.201	7

Fasanella & Sundararaghavan used DGEBA and DDS as a resin system and functionalized single wall carbon nanotube as a reinforcement material. They used the dendrimer growth approach to create the network structure which overcomes the limitation of one-step curing where overtrained structure may form as shown in Figure 10a,b [52]. This method also overcomes the limitation of multistage curing which is based on the cut-off distance criterion which goes on increasing during the equilibration process. In the dendrimer approach, thermoset resin was modeled by a single



monomer cross-linked to the second layer of monomers around it and so on. In this way, generations of monomer layers were added which led to the final structure being artificially introduced network strain due to step curing being avoided and the computational cost was also reduced. They observed isotropic properties in the final structure in all directions through MD simulation. With the addition of F-SWCNT they found that there was a significant improvement in elastic modulus whereas there was a decrease in coefficient thermal expansion as temperature increased

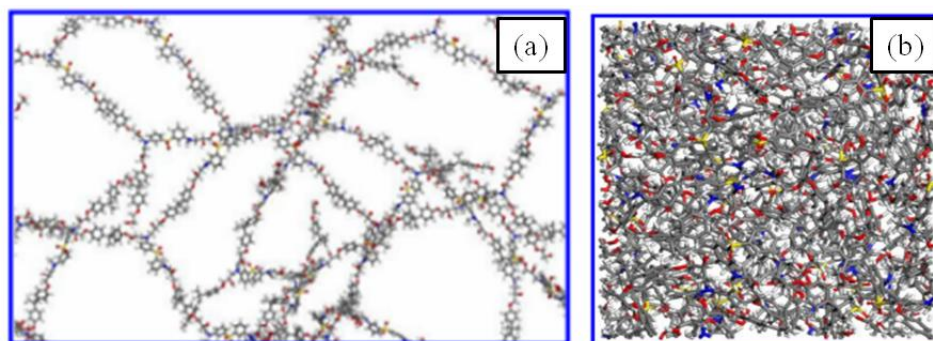


**Figure 10.** The dendrimer structure before (a) and after (b) energy Minimization (Reprinted from Ref. [52] with permission).

Polytrizoleketone(PTK) and polytrizolesulfone (PTS) with a different epoxy system like DGEBA or DGEBA with 3,30-diamino-diphenyl sulfone as a curing agent was studied for fracture toughness improvement [53]. They observed that there was a significant improvement in fracture toughness with moderate improvement in tensile strength as shown in Figure 11 with the addition of PTK/PTS. Table 2 shows the obtained results of the tensile properties of different samples. Due to high crosslinking material becomes highly brittle and there was a need to increase in fracture toughness for aerospace application of such resin system, the reason attributed for improvement in fracture toughness in this resin was when compared with other epoxy systems was immiscibility low of molecular weight PTS or PTK with other solid-state resins. From this discussion, they concluded that if a proper selection of resin and percentage with the addition of PTK/PTS there were improvements in fracture toughness. Here there is a need to carry out experimentation for different combinations of epoxy systems with varying weight percentages which is a tedious process hence MD simulation will be a better option to investigate reason so that proper combinations can be selected.

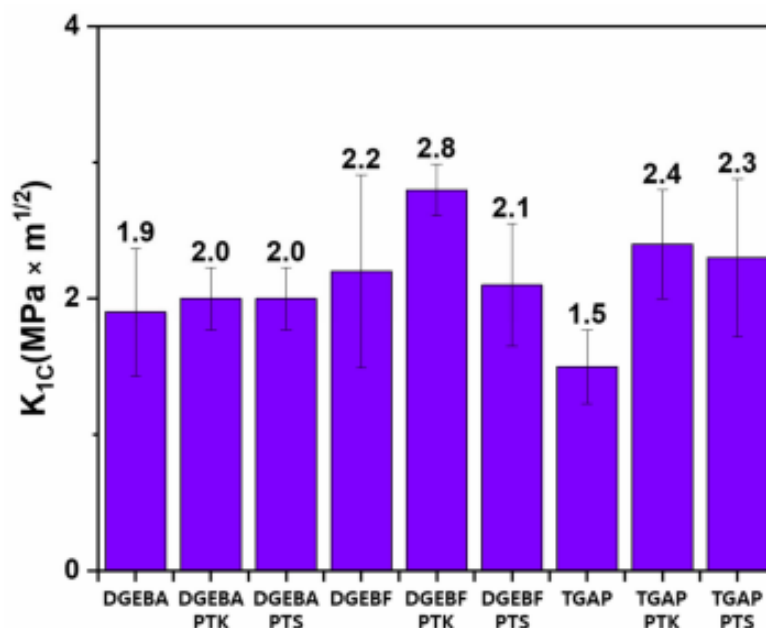


**Figure 11.** Fracture toughness of different combinations of the prepared samples [53].

**Table 2.** Tensile properties of the prepared samples [53].

Epoxy sample	Tensile strength (MPa)	Tensile modulus (MPa)
DGEBA	93.5 ± 13.7	1109 ± 173
DGEBA/PTK	89.3 ± 6.4	1032 ± 142
DGEBA/PTS	94.1 ± 4.2	1120 ± 29
DGEBF	86.3 ± 3.4	995 ± 33
DGEBF/PTK	93.7 ± 15.0	1052 ± 157
DGEBF/PTS	100.9 ± 6.0	1107 ± 127
TGAP	116.7 ± 8.2	1259 ± 140
TGAP/PTK	100.9 ± 10.6	1126 ± 129
TGAP/PTS	111.6 ± 11.9	1313 ± 151

Al Mahmud et al. did the multiscale modeling of carbon fiber/graphene nanoplatelets/epoxy (CF/GNP/epoxy) nanocomposites to find their mechanical properties by using reactive force field parameters in MD simulation [54]. The isotropic properties obtained from the MD simulation were assigned to GNP/epoxy repeating unit cell. Such eight subunit cells were taken to match the volume fraction GNP in epoxy of GNP/epoxy hybrid composite. Mechanical properties of this were evaluated using a generalized method of the cell as mentioned by Jacob et al. [55]. In micromechanics of composite materials, a generalized multiscale analysis approach was adopted. They observed improvement in axial modulus due to carbon fiber (CF), and also improvement in transverse modulus due to GNP. The multiscale modeling procedure adopted was shown in Figure 12.

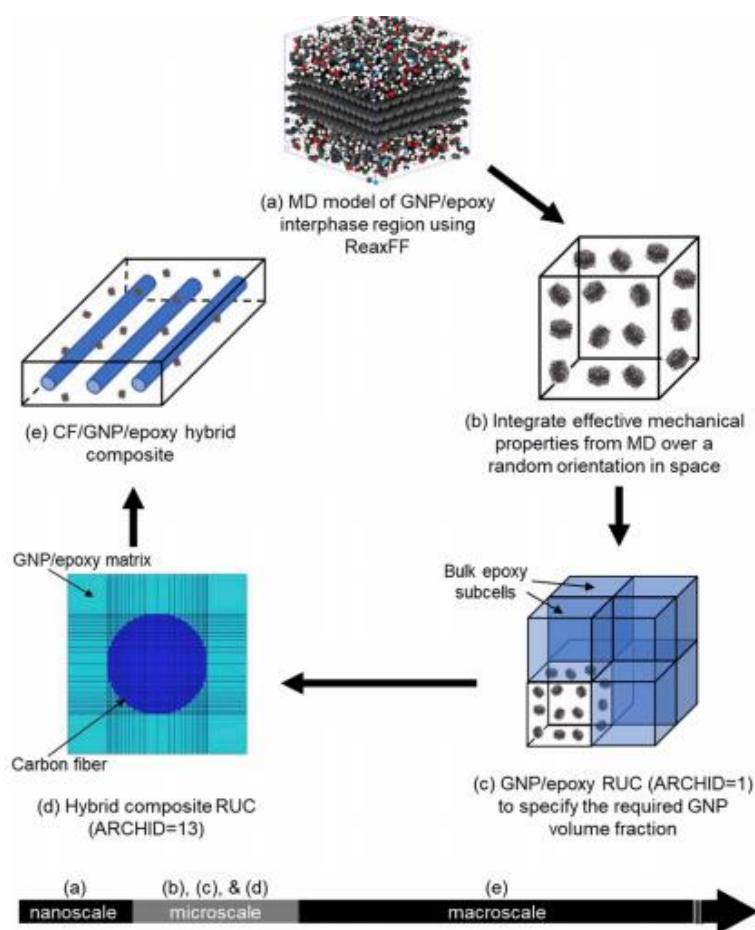


**Figure 12.** The multiscale modeling workflow for nanoscale to macroscale (Reprinted from Ref. [54] with permission).

Pramanik et al. proposed that a well-defined nanotube structure and methods to monitor the polymerization process at the molecular level will be a great promising approach for improvements in mechanical properties to achieve the theoretically predicted value of composite [56]. Detailed studies and a database of it are needed which include types of CNTs, polymers types, and interphase properties of these different combinations of polymers-CNTs, both theoretically and experimentally. They also found in the literature that functionality of the surface for covalent bonding leads to improvement in the interfacial shear strength of nanocomposite.

Aluko et al. studied the effect of the geometry of the CNT on its mechanical properties under different loading conditions [57]. Where they observed that the zig-zag configuration of CNT was a good option for the improvement of mechanical properties.

The MD simulation study was done to understand the effect of grafting the CNT on polyethylene terephthalate (PET) surface with a different configuration of CNT as shown in Figure 13 [58]. According to this study, controlling inter-tubular crosslinking and optimization of it will be a promising strategy to improve the strength of the MWCNT/PET composite. The author used the Hildebrand solubility parameter to design the solution of functionalized CNT so the proper exfoliation and dispersion of CNT in the polymer will happen, which was the most important criterion for manufacturing smart sensor materials. The alteration by covalent grafting of nanotube

improves interfacial load transfer from the PET matrix to nanotubes and vice versa since it reduces the stiffness of CNT more than pristine CNT. To control the properties of the smart nanocomposite covalent grafting on the CNT's lateral surface and the grafting ratio was an important criterion.

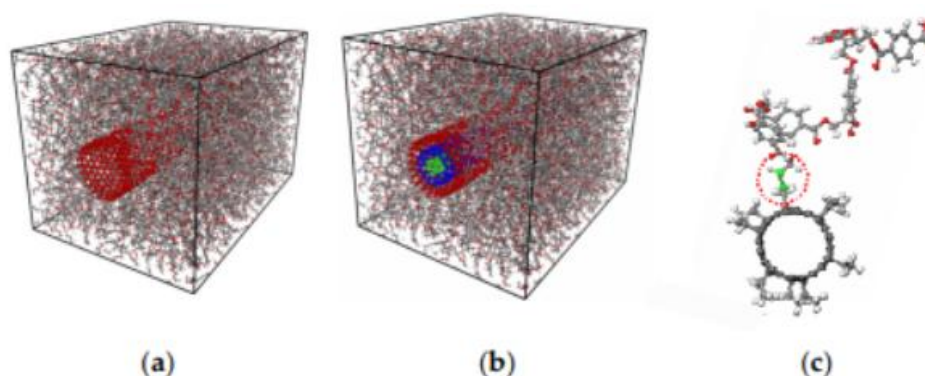


**Figure 13.** (a) Molecular models of grafting SWCNT in SWCNT/PET nanocomposites, (b) Molecular models of grafting MWNT in MWNT/PET nanocomposites, (c) covalent grafting of CNT and PET molecules [58].

Zhu et al. proposed an extension to the Mori-Tanka micromechanics model to predict the effect of CNT waviness on the effective properties of the interface between CNT/epoxy nanocomposite and interfacial damage [59]. They used the MD simulation for this since it accounts for the van der Waals and electrostatic forces due to the waviness of CNT.

Subramanian et al. investigate the cohesive behavior by studying traction-separation law when it was subjected to mechanical loading of carbon fiber/CNT/epoxy nanocomposite [60]. The interphase model generated for MD simulation has voids in multiple graphene layers which enables them to simulate physical entanglement between the polymer and the carbon fiber surface. Here they used the cohesive zone modeling (CZM) approach to model the different constituents in the considered composite. CZM approach adopted allows the interface debonding modeling for the prediction of debonding issues in pristine interfaces. The pull-out test result shows that the elastic region under displacement load was because of the polymer chains stretching and sudden hardening was due to the entanglement of polymer chain under further stretching as shown in Figure 14. This entire mechanism leads to propose of the effective load transfer between the polymer chains, CNT, and the carbon fiber. The intermediate fluctuations in the stress-strain curve were represents the chain breakages in regions of poor epoxy crosslinking density.

A study on the effect of contact angle on the effective wettability of CNT and carbon surface and different epoxy resin by using MD simulation was done [61]. The Study reveals that the length of the monomer chain, temperature, and the reactive sites in the monomer has a significant impact on the contact angle values on the CNT surface. They found that di-functional resins have best the wettability such as DGEBA/DETDA, but the glass transition temperature of this combination was comparatively low because of which wettability decreases at higher temperatures.

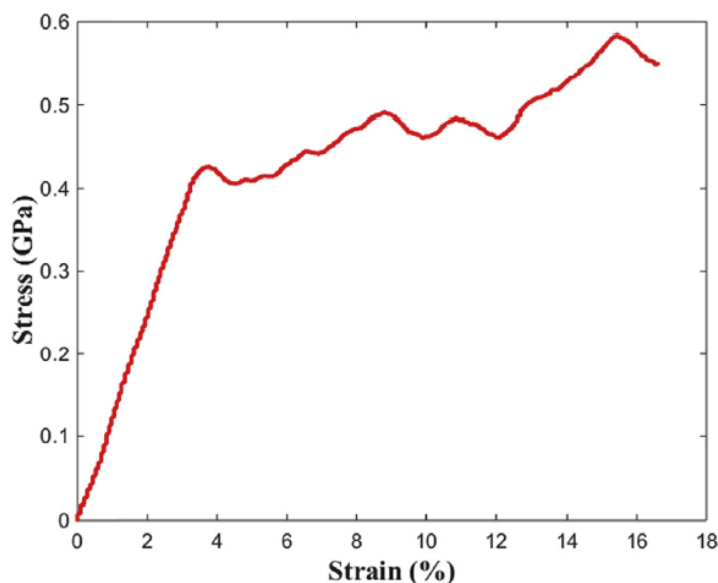


**Figure 14.** Stress-strain response during interphase pullout test (Reprinted from Ref. [60] with permission).

## 6. Molecular dynamics techniques for thermal characterization of polymeric nanocomposites

In the case of all polymeric nanocomposite glass transition temperature ( $T_g$ ) is one of the most important parameters over which the selection of polymer for different applications depends on. The value of  $T_g$  well above room temperature is an indicator of resin suitable for structural application. Therefore, the prediction of the value of  $T_g$  is the key factor while designing new materials. Along with  $T_g$ , some other thermal properties are also important like the coefficient of thermal expansion (CTE), thermal aging, the effect of cross-linking density on thermal and mechanical properties which are to be addressed.

Bandyopadhyay et al. proposed a method for the development of a large system of EPON 862 and DETDA molecules [62]. They used both molecular dynamics and molecular mechanics approaches for the creation of EPON-DETD structure with a 2:1 molecular ratio with the static cross-linking method. The density-temperature plot (Figure 15) shows a characteristic change in slope in the glass-transition temperature region. Further decrease in temperature below glass transition temperature marks no significant decreases in the polymer structure's free volume which concludes that no further crosslinking was possible since no reactive sites were present on the polymer chain within the specified cut-off distance. For the 54% cross-linking density structure, the value of  $T_g$  was found in the range of 80 to 100 °C. For the 76% cross-linking density structure, the  $T_g$  was found to be in the range of 90 to 110 °C which reflects that with the increase in cross-linking density there was a significant improvement in the glass transition temperature range.

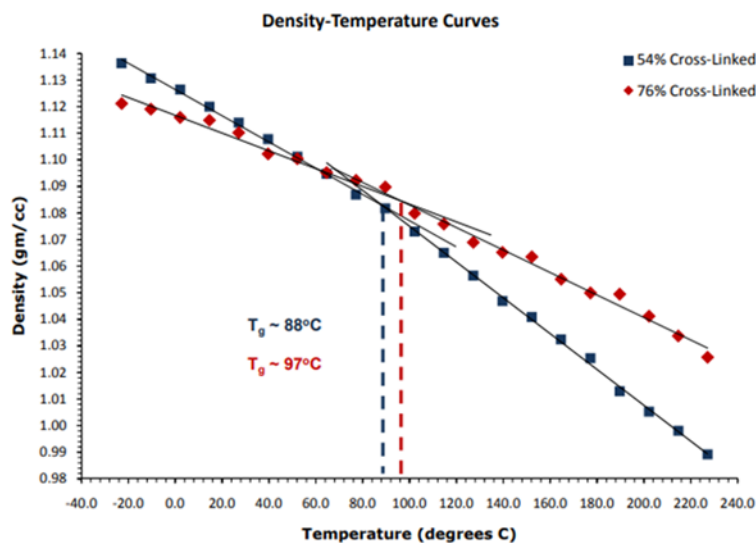


**Figure 15.** The dependence of the crosslink density on cross-linking cutoff distance [62].

A study was done on molecular modeling of physical aging in epoxy polymers which can help to predict thermo-mechanical properties of aged epoxy and which acts as a guiding tool for the design of durable composite materials [63]. Physical aging of polymeric material was observed when it was exposed to temperatures below the glass transition range ( $T_g$ ) for extended periods of time which can be characterized by an increase in mass density and/or a decrease in energy associated with molecular conformation of polymeric materials. The author developed a number of stable cross-linked molecular models of the EPON 862-DETDA which acts as an unaged (baseline) state of the epoxy with various crosslink densities. As the physical aging process could not be directly simulated for the type of MD models under consideration, an approach was developed to establish a relationship between the aging time of the polymer and the corresponding change in specific volume shrinkage of the MD simulation box for a particular value of aging temperature. The aging temperature versus changing volume relationship was developed which is useful for the determination of any state of aging, characterized by a particular aging temperature.

Epoxy resin Di-glycidal ether of Bisphenol-F, Epicure curing agent nanocomposites reinforced with three different ionic liquid functionalized carbon nanotubes (f-CNTs) was fabricated by an in-situ polymerization method [64]. They studied the curing process under the influence of the anions through DSC and normalized FTIR spectroscopy techniques and the final composition was analyzed by X-ray photoelectron spectroscopy. The tensile strength was increased dramatically due to the insertion of f-CNTs. The effects of the anion from ionic liquids on the curing behavior of an epoxy show that the PF6-CNT/epoxy nanocomposites and neat epoxy have the same curing process, whereas Cl-CNT and Br-CNT/epoxy nanocomposites were affected by the halogen anions in the curing. In comparison of the degree of curing in all these three cases, they suggested that the cure mechanisms of the Cl-CNT and Br-CNT samples were different than neat resin and PF6-CNT/epoxy composites. Ionized liquid-CNTs show considerable improvement of the DC conductivity at a lower weight percentage of CNTs and tensile strength also significantly improved compared with other carbon nanotube-based fillers.

Hadipeykani et al. carried out an MD simulation to study the effect of CNT diameter, the

volume fraction of CNT, and the chirality of CNT on glass transition temperature, coefficient of thermal expansion of the nanocomposite [65]. They found that the prediction of  $T_g$  and coefficient of thermal expansion of nanocomposite were in good agreement with previous studies. They observed that as the diameter of CNT increases the value of  $T_g$ , and CTE value was increased.  $T_g$  and CTE of the nanocomposites decrease with a reduction in the volume fraction of CNT in nanocomposites when the diameter and type of CNT were kept constant. When armchair CNT was used instead of zigzag CNT in nanocomposites, the  $T_g$  of nanocomposites decreases, and the CTE increases, when the weight fraction of CNT was kept constant.

The coarse grain MD simulation for demonstrating the dependency of gel point,  $T_g$ , and the morphology of the epoxy on how the curing has occurred studied by Henry et al. [66]. They also validate their result for 44DDS/DGEBA/PES epoxy system experimentally.

Crawford et al. quantify the effect of polymer blend on its thermal properties to predict its cure kinetics and try to optimize the simulation time, model size, and hysteresis effect of the model so that near accurate results of the experiment can be mapped with MD simulation [67].

Hall et al. emphasize on the model building of three different epoxy monomers so that real mimicking the actual systems of the resin curing process for the prediction of the glass transition temperature [68]. Here they used two types of epoxy monomers, i.e., DGEBF and triglycidyl-p-amino phenol (TGAP) with the curing agent diamino diphenyl sulphone (DDS). They produced different models with oligomers and monomers of pure epoxy so that an exact representation of the real epoxy mixture can be produced based on epoxy equivalent weight which represents the exact real epoxy structure. They carried out the MD simulation with fewer monomers, and dimers of DGEBF so that the exact purity of the resin which was supplied by the supplier can be matched.

Koo et al. did a study on the glass transition temperature of smart epoxy composite made of DGEBF, DETA in the ratio of (100:27) and tris-(cinnamoyloxymethyl)-ethane (CTE) 10% of the total weight of the neat epoxy unit cell [69]. The influence of the use of smart material (stress-sensitive material) on the cross-linking degree and  $T_g$  epoxy has been investigated numerically and experimentally. They also observed that there was a reduction in  $T_g$  value with the addition of smart material to neat epoxy which can help design smart epoxy composites.

Sul et al. [70] develop a new methodology by using atomistic modeling and MD simulation for the generation of resin systems whose properties such as dilatation caused by the constraining effect of the fibers at high temperatures during curing. This methodology can be used as a guiding tool during the continuum level to influence the design of a material system. With the addition of SWCNT, they observed that there was a reduction in the coefficient of thermal expansion and glass transition temperature attributed it as, at high-temperature annealing intermolecular forces were reduced.

A comparative study done by different researchers on the basis of different computational studies done on the basis of computational tools used, type of nano filler used and properties evaluated was mention in the Table 3.

**Table 3.** Different comparative analysis of different computational studies done on the basis of computational tools used, type of nano filler used and properties evaluated.

Form of nanoparticle	Polymer matrix	Interatomic potential/FF	Properties evaluated	Refs.
-	EPON 862 and DETDA	OPLS United Atom force field	Effect of different cross linking density on glass transition temperature	[1]
CNT (filament type)	(DGEBA), (DGEBF), (TGDDM)	CHARMM	Effect of interaction between different epoxies and CNT was studied.	[28]
single-walled CNTs (5, 5), respectively, with the diameters of 6.78 Å and 13.56 Å	Polycarbonate	(COMPASS) force-field	Effects of weight fraction and aspect ratio of CNTs on the elastic properties of PC/SWCNT nanocomposites.	[71]
SWCNT with different configuration	polythiophene(PT)/polyethylene (PE)/poly(p-phenylenevinylene) (PPV)	ReaxFF	Influence of CNT diameter, polymer type, and temperature on interaction energy and also the found relation between mechanical properties and interaction energy.	[37]
TEOs Electrospun Nanofiber (0.2–0.8%)	EPON 862(DGEB-F)/w resin system		Adding 2 g by weight nanofibers increased both tensile strength, modulus of the composite by 14% and 5%.	[72]
Carboxyl-modified multi-walled carbon nanotubes (MWCNT–COOHs)	diglycidyl ether of bisphenol A (DGEBA) toughened with carboxyl-terminated butadiene-acrylonitrile (CTBN)		Activation energy of rubber-toughened epoxy nanocomposites decreased with the increasing of MWCNT–COOH contents. The maximum tensile and flexural properties were obtained at MWCNT–COOH concentration of 0.5wt% with uniform dispersion. Glass transition temperature of rubber-toughened nanocomposite decreased with the increasing MWCNT–COOH contents.	[73]
GFRP, 1 wt%, 1.5wt%, 2 wt% of TEOS ENFs	EPON resin 862/EPIKRE W		1%, 1.5% and 2 wt% TEOS ENFs and GFRP composite were compared and it was observed that, the flexural strength and flexural modulus were increased by 14% and 8% with 2 wt% of TEOS ENFs. Increase in the energy absorption, and was found to be 19%, 55%, and 93% for 1%, 1.5% and 2 wt% of TEOS ENFs	[74]
CNT's	Methyl methacrylate (PMMA)	COMPASS force-field	Young's moduli of the interfacial region and composite. Effect of the aspect ratio of CNT's on mechanical properties.	[38]

*Continued on next page*



Form of nanoparticle	Polymer matrix	Interatomic potential/FF	Properties evaluated	Refs.
--	(DGEBA as resin and (DETA) as curing agent	COMPASS, PCFF, UFF and Dreiding	Young's modulus, shear modulus, bulk modulus, Poisson's ratio, Density were evaluated and found that COMPASS and PCFF force field result are more reliable and matches with experimental results.	[39]
	DGEBA and hardener DETDA	COMPASS force field	The influence of model size, extent of curing and length of epoxy strands on the thermo-mechanical properties of epoxy-based polymer networks. Static deformation approach allows to calculate elastic constant compensated for the large scattering of the mechanical properties data due to nanoscopically small volume of simulation cells.	[41]
SiC nanoparticle	DGEBF and hardener TETA	polymer-consistent force field (PCFF) potential	The methodology yields an effective volume fraction and mechanical properties of the interphase in a nanocomposite system. The effective interphase thickness of the equivalent continuum model increases with the particle radius scale Increase of the nanoparticle curvature also leads to a larger non-bond interaction space and generates a stiffer interphase layer. Mechanical properties of the interphase are improved as the particle size is decreased, while the layer thickness is reduced.	[42]
-	DGEBF and hardener DETDA	OPLS	Physical aging of composite at a temperature 40 °C bellow $T_g$ , relation between the aging time and corresponding change in conformal structure and observed that volume reduction and mass density increase.	[63]
0.1, 0.5, 1% F-CNT	DGEBF and hardener DETDA	-	Mechanical and electrical properties of nanocomposites with fictionalized CNT as nano filler. Fracture surface analysis shows strong interfacial bonding between the carbon nanotubes and the polymer matrix. Curing kinetics to find $T_g$ also studied by DSC and find degree of curing.	[44]
-	DGEBF and hardener DETDA	OPLS	Relation between $T_g$ and coefficient of thermal expansion for different crosslinking density and dependence between the crosslinking density and cut of distance were evaluated.	[64]

*Continued on next page*

Form of nanoparticle	Polymer matrix	Interatomic potential/FF	Properties evaluated	Refs.
SWCNT	DGEBF and DETDA	COMPASS	Found the tensile strength of SWCNT to be around 1.4 TPa by using MD simulation.	[43]
Coiled CNT			Coiled MWCNT were produced which can used for the improvement of nanocomposite properties.	[44]
6%, 8%, 10% SiO <sub>2</sub> Nano particles	DGEBF and hardener TETA	Compass II	Bulk modulus and Share modulus were calculated with different weight fraction of SiO <sub>2</sub> nanoparticles.	[75]
7%, 12% SWCNT	DGEBF and hardener DETDA	COMPASS force field	Effect of carbon vacancy defects on the mechanical properties epoxy/SWCNT nanocomposites. As defects increases the Young's modulus decreases.	[46]
CNT (10, 10), CNT (15, 15), CNT (10, 0), CNT (15, 0)	DGEBA and hardener DETA	COMPASS27	The effect of CNT diameter, CNT volume fraction, chirality on T <sub>g</sub> and CTE of nanocomposite were studied and found that as diameter increase T <sub>g</sub> increases.and CTE also increases.	[65]
CNT	DGEBF and hardener DETDA	COMPASS	Machine learning frame work was developed based on MD simulation data for the predication of critical pull-out force and CNT/epoxy interfacial strength.	[47]
-	DGEBF and hardener 44DDS	OPLS 2005	Effects of competitive primary and secondary amine reactivity of hardener on the structural evolution and properties of an epoxy thermoset resin during cure.	[76]
Graphene	DGEBF and TETA systems	COMPASSII	Used shear deformation model to determine interfacial shear modulus of graphene and epoxy interface.	[49]
-	44DDS/DGEBA/PES	OPLS-2005	Done force field parameterization and validate the MD simulation results with experimentation results for reaction kinetics. Predicted MD results of degree of cure, gel-points, and morphology predictions were validated against experimental results.	[66]
-	Cyanurate polymer	PCFF	Effect of blends of Cyanurate polymer on its properties.	[67]
-	DGEBF, TGAP and DDS as hardner	PCFF	Emphasis on model building epoxy monomers so that real mimicking the actual systems with desired purity.	[68]
-	DGEBF, DETA (100:27) and CTE 10% of the total weight of the neat epoxy unit cell	MMFF	Carried out MD simulation smart epoxy stress sensitive composite material for the prediction of glass transition temperature and crosslinking density.	[69]

*Continued on next page*

Form of nanoparticle	Polymer matrix	Interatomic potential/FF	Properties evaluated	Refs.
	DGEBF, DETA, CTE	MMFF	Carried out MD simulation and used in development of spring-bead network model through parametric studies and mechanical equivalence optimization to represent the microstructure of the material and macroscopic mechanical properties were calculated by multiscale approach.	[48]
	Spyros V. Kallivokas	Dreiding force field	MD simulation of four different cross linking structures were done to study the topological behavior of crosslinking, dynamic local volumetric changes and density changes through different simulation approach which were in good agreement with experimental XRD results from the literatures.	[50]
GNP, CNT	DGEBA, and DETA	COMPASS	Experimental analysis and multiscale modelling based on molecular dynamics simulation carried out to determine mechanical properties of carbon nanotube and graphene nanoplatelet hybrid nanocomposites. Elastic constants of these molecular samples were converted to microscale values using equivalent fiber method with a three-stage algorithm	[51]
F-SWCNT	DGEBA-DDS	CVFF	Thermal and mechanical properties of cured epoxy resins reinforced with pristine and covalently functionalized SWCNT. They observed that increase in stiffness value with decrease in coefficient of thermal expansion when compared with pristine SWCNT/epoxy nanocomposite.	[52]
-	(DGEBA, DGEBF, and TGAP) with 3,30 –DDS and PTS, PTK as toughening agents	-	Studied the toughening effect by addition of polytrizoleketone (PTK) and polytrizolesulfone (PTS) with different epoxy system like DGEBF or DGEBA with 3,30-diaminodiphenylsulfone as a curing agent. Observed improvement in toughness.	[53]

*Continued on next page*

Form of nanoparticle	Polymer matrix	Interatomic potential/FF	Properties evaluated	Refs.
CF, GNP	DGEBF, DETDA	ReaxFF	Attempted for multiscale modeling of CF/GNP/epoxy hybrid composites for mechanical property evaluation by using ReaxFF force field parameters. The predicted properties of the GNP/epoxy composite were used as the matrix properties to generate a representative unit cell of the CF/GNP/epoxy hybrid composite. They observed improvement in axial modulus due to carbon fiber (CF), and also improvement in transverse modulus due GNP.	[54]
SWCNT	(DGEBA (44DDS)	COMPASS	Develop a new methodology by using atomistic modeling and MD simulation for generation of resin system which can improve the high temperature annealing performance of composite material.	[70]
SWCNT	DGEBF, DETDA	OPLS, ReaxFF	Effect of chirality of the CNT on mechanical properties was studied. Modulus in the axial direction of the CNT was observed to improve significantly when Zig-Zag configuration of CNT was taken.	[57]
SWCNT with a chirality of (23, 0) and a MWNT consisting of three SWCNTs with chiralities of (23, 0), (14, 0), and (5, 0)	polyethylene terephthalate (PET)	PCFF	Effect of covalent grafting the CNT on PET will improve the interfacial properties and increase the stiffness on the nanocomposite.	[58]
SWCNT	DGEBF, TETA	COMPASS and PCFF	Effect of CNT waviness on the effective properties of nanocomposite by using extended Mori Tanka model.	[59]
Carbon fiber, CNT	DGEBF, DETA	OPLS, MMFF	Evaluated the interfacial properties of multiscale reinforcement in carbon fiber CNT/epoxy nanocomposite.	[60]
Sudo aromatic carbon surface	BMPM and DABPA, Bisphenol-A Benzoxazine, DGEBF and DETDA, TGMDA and DDS, Fluorinated cyanate ester, nonfluorinated cyanate ester	IFF	Wettability of the carbon fiber with different resin with temperature variation was studied by using MD simulation.	[61]
Bone-shaped SWCNT, and single-walled carbon nanotubes	Polyethylene	Dreiding generic force field	Novel bone shaped single wall carbon nanotube model was proposed and effect of its incorporation of stiffness, tensile, and yield stress in Polyethylene matix at different temperature was addressed. To have comparisons results were compared with capped single wall carbon nanotube reinforced polyethylene nanocomposite.	[77]

## 7. Multiscale modeling approaches for polymer nanocomposites

Despite the importance of understanding material properties and molecular structures, their behavior can be made consistent with respect to different aspects at different scales. Macroscopic behavior is generally described without considering individual atomic and molecular structures. It is also based on the assumption that the material is continuously distributed throughout its volume, resulting in an average density and subject to the surface and gravitational forces. Macroscale or continuum methods obey (i) the fundamental law of continuity based on the conservation of mass; (ii) Momentum considerations and equilibrium based on Newton's second law; (iii) Momentum principle; (iv) Conservation of energy derived from the first law of thermodynamics; (v) Conservation of entropy derived from the second law of thermodynamics. Continuum models based on these laws must be combined with appropriate constitutive laws.

Micromechanical techniques are used to describe continuum quantities associated with very small material elements in terms of the structure and behavior of micro components due to the mismatch in the mechanics of the microscale continuum. Therefore, the properties of the local continuum are statistically represented by developing a representative volume element (RVE) of the micromechanical model. RVE is constructed to check the consistency of length scales with minimal components that have first-order effects on macroscopic behavior and is further used in 1:1 scale models. Micromechanical techniques can represent the interface between discontinuities, components, and coupled mechanical and non-mechanical properties.

### 7.1. Finite element modeling

Finite element method is a powerful numerical analysis tool used to observe the mechanical behavior of composite material that was started in the 1970 decade and then number of models are developed to analyze different composites [78]. Carbon nanotubes (CNTs), which provide excellent strength and stiffness along with better thermal and electrical properties, were discovered by Sumio Iijima, a Japanese scientist in 1991 [79,80]. CNTs were utilized as reinforcing elements to develop nanocomposites. Recently, there has been explosively experimental and analytical work carried out along with finite element modeling on analyzing, developing and characterizing CNT reinforced polymeric nanocomposites and other nanocomposites. Finite element modeling approaches are multi-scale RVE, object oriented and unit cell modeling.

#### 7.1.1. Multiscale RVE modeling

Li and Chou [81] extended the RVE concept at the nanoscale and assessed the essential mechanical properties of CNT reinforced polymer composites with the help of 3D nanoscale RVE depending upon finite element and elasticity theory. In RVE, nanofiller (e.g., carbon nanotube) is surrounded by a matrix and suitable boundary conditions are applied to represent the effects of matrix material. In the multi-scale modeling technique, to observe the compressive strength of nano polymer composites, a nanotube is modeled at the atomistic scale and analyzed for matrix deformation using the continuum finite element method. Truss rods were used to simulate the Van der Waals interactions between carbon atoms and the finite element nodes of the matrix. Zhang related atomistic simulation with continuum analysis by combining inter atomic potential and CNTs atomic structures into constitutive laws. Shi et al. [82] studied the mechanical performance of CNTs surrounded by matrix material in composites by exhibiting a combined atomistic and continuum mechanics technique. Representative volume cells are obtained by modified Morse potential and

progressive fracture model.

Multiscale RVE incorporates continuum and nanomechanics to bridge the gap between length scales from the nanoscale through the mesoscale. Bagha and Bahl [83] used square representative volume (RVE) cells in finite element analysis to predict the mechanical properties of vapor grown carbon fiber (VGCF) reinforced nanocomposites and compared results with the conventional rule of mixtures. They considered two types of arrangement inside the RVE, mainly VGCF inside the RVE and VGCF through RVE. Tserpes et al. [84] presented a multi-scale RVE to observe the tensile properties of CNT polymeric composites in which rectangular representative cell, whose total volume is filled by the matrix material, is modeled by 3D solid elements, while a nanotube is modeled by 3D beam element. Sanei et al. [85] generated computer-simulated microstructures at different length scales to observe change in elastic properties and their results were used to determine RVE size for multiscale analysis. They concluded that RVE is mainly dependent on material properties and microstructure type. Figure 16 shows the synthesis of the RVE. The RVE is synthesized in two steps. (i) Progressive fracture model [86] is used to simulate the behavior of the isolated nanotube. The model concept is based on the assumption that CNTs act like space frame structures under loading. Member joints are represented by carbon atoms and a bond between carbon atoms represents load-carrying members. Modified Morse potential is used to model the non-linear behavior of carbon-carbon bond and FEM is used to model CNT's structure. (ii) RVE is formed by inserting nanotubes into the matrix. Matrix material and nanotubes are modeled by solid and 3D elastic beam elements respectively. The representative RVE of the composite systems generated for FEA is shown in Figure 17. The flow chart in Figure 18 presents the process of RVE generation for FEA.

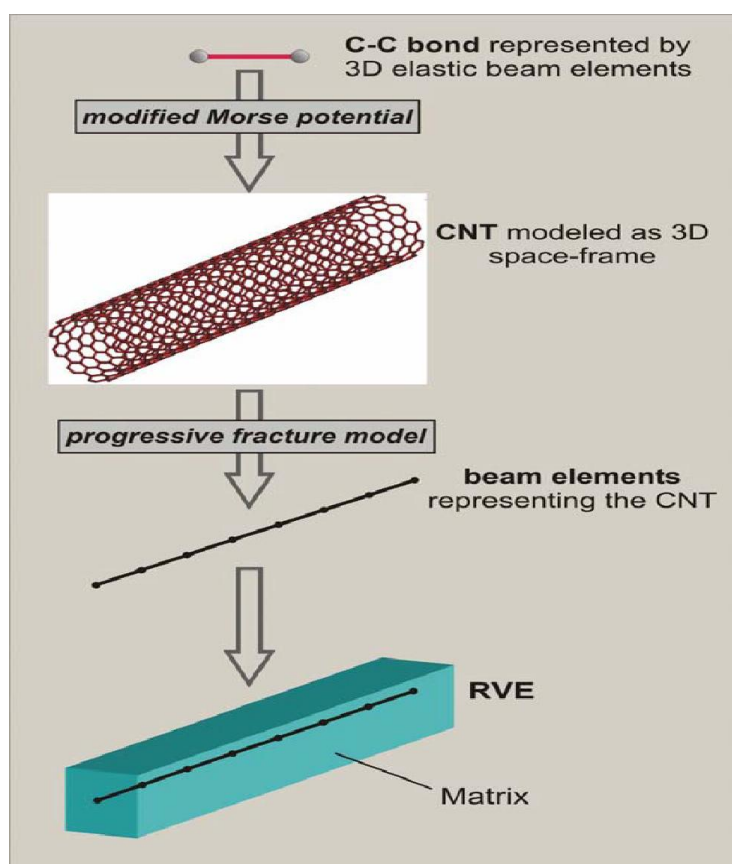


**Figure 16.** RVE synthesis (Reprinted from Ref. [87] with permission).

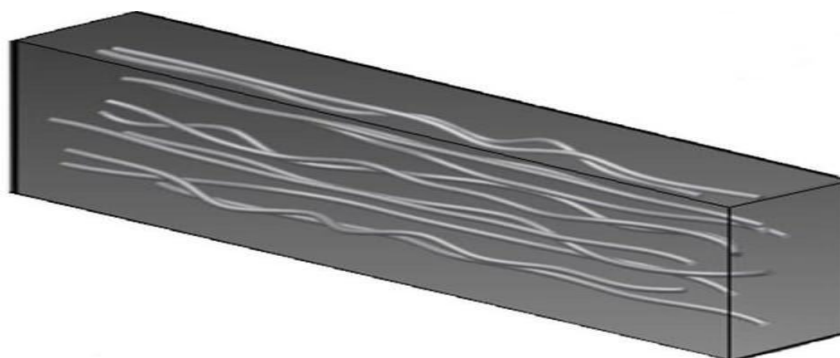


**Figure 17.** RVE generated for FEA reinforced with CNT (Reprinted from Ref. [88] with permission).

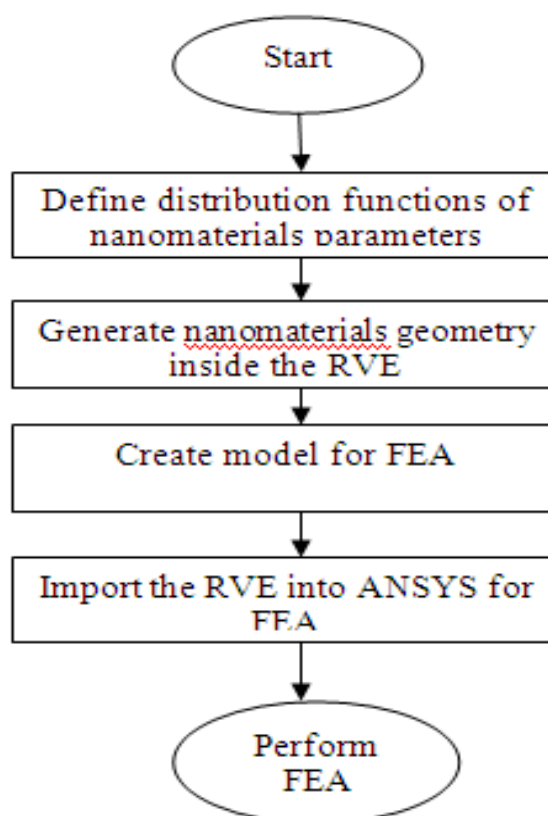


**Figure 18.** Steps used to generate RVE for FEA (Reprinted from Ref. [88] with permission).

### 7.1.2. Unit cell modeling

Ordinary unit cell modeling is similar to multiscale RVE modeling. Unit cell is considered as a special RVE of relatively large and definite size and contains sufficient filler count. It is difficult to form analytical models for such a defined unit cell due to its complexity, and numerical technique and simulation become essential. Finite element method is a widely used method to analyze the mechanical behavior of nanocomposite with unit cell [87].

### 7.1.3. Object-Oriented modeling

Multi-scale RVE and unit cell modeling are based on assumptions. These assumptions are, nanofillers can be considered as cylinders, spheres, cubes or ellipsoids and a number of unit cells or

RVEs can be assembled to reproduce nanocomposites. Assumption holds good for simple and homogeneous nanocomposites. The object-oriented modeling is used to overcome the drawbacks of multiscale RVE modeling and unit cell modeling. For example, for irregular filler geometry it's difficult to capture size, morphology and reinforcement displacement. In such cases, a relatively new approach, which can capture nanocomposites actual microstructure morphology, becomes essential to predict properties and it is object-oriented modeling. It incorporates micrographs into finite element grids. Mesh reproduces the original microstructure [88]. Chou et al. [81] evaluated the mechanical behavior of SiC particle-reinforced Al composites by using 3D object-oriented finite element modeling. The result of the modulus of elasticity based on object-oriented models has shown good agreement with the experimental and numerical results based on simplified models like prisms, spheres and ellipsoids.

Figure 19 shows some sample results. As compared to simple analytical models, 3D microstructure-based models can predict properties of particle reinforced composite properties more accurately, as analytical models do not consider microstructural factors which affect mechanical performance of the material.

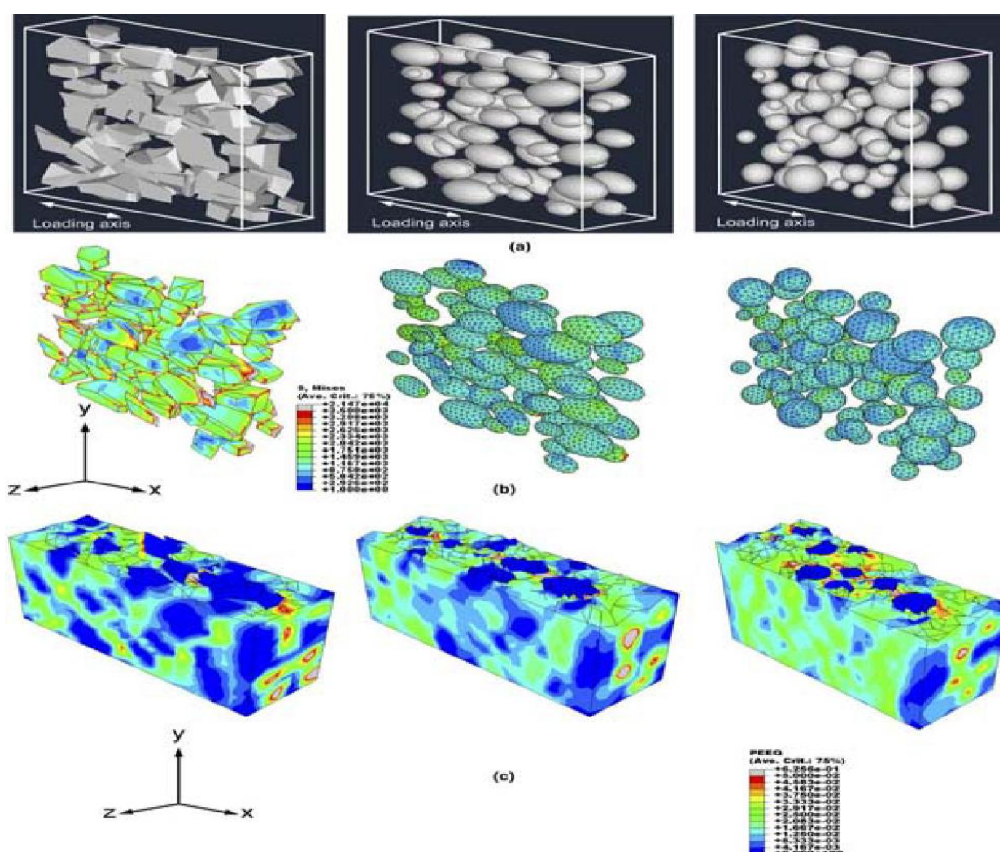


**Figure 19.** (a) Finite element models containing actual and approximated spherical particles, (b) Distribution of Von Mises Stress and (c) Strain (Reprinted from Ref. [89] with permission).

The finite element method is used in this work to perform a buckling analysis of laminated composite rectangular plates reinforced with multi-walled carbon nanotube (MWCNT) inclusions using FEM [90]. To compute the elastic modulus of the nanocomposite matrix, the law of mixtures and the Halpin-Tsai model are used. Three key elements, including the effects of random dispersion, waviness, and agglomeration of MWCNTs in the polymer matrix on the material characteristics of the



nanocomposite are investigated. The critical buckling loads of the composite plates are then numerically computed for various design parameters such as plate side-to-thickness ratio, elastic modulus ratio, boundary conditions, layup schemes, and fiber orientation angles. The effect of carbon nanotube fillers on the critical buckling stress of a nanocomposite rectangular plate, taking into account the changes.

Elastic-mechanical properties of graphene monolayer-based nanocomposites considering hybrid interface region addressed by using FEM [91]. The interfacial area between reinforcement and matrix is analyzed using multi-scale finite elements approach. At the first level of analysis, the proposed method uses an atomic representation of graphene. Extract its elastic-mechanical behavior. The output is then used in the second level of analysis. The representative volume element (RVE) of nanocomposites is considered. Modeled using continuum mechanics assumptions via the use of solid finite elements and intermediate phase known as interphase is approached using solid finite elements as well as a hybrid concept. According to this concept, it is considered the region between the two constituent materials' mechanical properties.

## 8. Conclusions

This review gives detailed insight into the use of molecular dynamics simulation techniques used by the different researchers for the characterization of polymeric nanocomposites. The main focus of this study was the thermal and mechanical characterization studies done for CNT/epoxy nanocomposite materials using MD simulation. Different studies show that by reinforcement of CNTs, mechanical properties were improved because of improvement in interfacial strength between epoxy and CNT. Various aspects like aspect ratio, weight percentage, morphology, size, shape, and defects in CNT were some of the reasons on which thermal and mechanical properties depended. Thus, molecular dynamics simulation will be the best route to study the molecular level phenomenon to understand the reasons for property variation in these materials. Glass transition temperature range of epoxy will change with the addition of CNT which may be one of the main criteria while thermal characterization of CNT/epoxy nanocomposites. MD simulation thus will be a major alternative for the evaluation of the thermal and mechanical properties of epoxy nanocomposites without carrying out time-consuming tedious experimentation. Very few studies were carried out by using multiscale reinforcement, especially on micro glass fiber reinforced with CNT in polymeric nanocomposites for the characterization of such materials. Also, very little work was done on three-phase polymeric hybrid nanocomposite which has two or more types of nano-reinforcement for their mechanical characterization.

The simulation techniques developed to date have their own pros and cons, depending on the issues addressed by the researchers. The molecular simulations address molecular interactions and structure on the scale of 0.1–10 nm. The result obtained can be used to understand the interaction strength at nanoparticle-polymer interfaces and the molecular origin of mechanical property improvement. Since, molecular simulations are computationally time-consuming, thus not directly applicable to the prediction of mesoscopic structure and properties such as the dispersion of nanoparticles in the polymer matrix and the morphology of polymer nanocomposites. To understand the effect of morphology on these scales, mesoscopic simulation methods like DPD and dynamic mean field theory are more effective. On the other hand, the macroscopic properties of materials are usually studied by the use of mesoscale or macroscale techniques such as micromechanics and FEM. But these techniques may have limitations when applied to polymer nanocomposites because of the difficulty to deal with the interfacial nanoparticle-polymer interaction and the morphology, which are

considered crucial to the mechanical improvement of nanoparticle-filled polymer nanocomposites. Thus as a concluding remark, new multiscale modeling approaches are to be developed which address all the issues at different times and scales.

### Conflict of Interest

The authors declared no potential conflicts of interest with respect to the research, authorship, and/or publication of this article

### References

1. Bandyopadhyay A, Valavala P, Clancy T, et al. (2010) Atomistic modeling of cross-linked epoxy polymer. *52nd AIAA/ASME/ASCE/AHS/ASC Structures, Structural Dynamics and Materials Conference 19th AIAA/ASME/AHS Adaptive Structures Conference 13th*, Denver, Colorado. <https://doi.org/10.2514/6.2011-1920>
2. Lefrant S, Buisson JP, Schreiber J, et al. (2004) Raman studies of carbon nanotubes and polymer nanotube composites. *Mol Cryst Liq Cryst* 415: 125–132. <https://doi.org/10.1080/15421400490482844>
3. Li X, Chen W, Zhan Q, et al. (2006) Direct measurements of interactions between polypeptides and carbon nanotubes. *J Phys Chem B* 110: 12621–12625. <https://doi.org/10.1021/jp061518d>
4. Rahmat M, Hubert P (2011) Carbon nanotube-polymer interactions in nanocomposites: a review. *Compos Sci Technol* 72: 72–84. <https://doi.org/10.1016/j.compscitech.2011.10.002>
5. Pielichowski K, Pielichowska K (2018) *II-Polymer nanocomposites, Handbook of Thermal Analysis and Calorimetry*, Elsevier, 6: 431–485. <https://doi.org/10.1016/B978-0-444-64062-8.00003-6>
6. Zeng QH, Yu AB, Lu GQ (2008) Multiscale modeling and simulation of polymer nanocomposites. *Prog Polym Sci* 33: 191–269. <https://doi.org/10.1016/j.progpolymsci.2007.09.002>
7. Zhao J, Wu L, Zhan C, et al. (2017) Overview of polymer nanocomposites: Computer simulation understanding of physical properties. *Polymer* 133: 272–287. <https://doi.org/10.1016/j.polymer.2017.10.035>
8. Lee JY, Baljon ARC, Loring RF, et al. (1998) Simulation of polymer melt intercalation in layered nanocomposites. *J Chem Phys* 109: 10321–10330. <https://doi.org/10.1063/1.477687>
9. Smith GD, Bedrov D, Li LW, et al. (2002) A molecular dynamics simulation study of the viscoelastic properties of polymer nanocomposites. *J Chem Phys* 117: 9478–9489. <https://doi.org/10.1063/1.1516589>
10. Smith JS, Bedrov D, Smith GD (2003) A molecular dynamics simulation study of nanoparticle interactions in a model polymer-nanoparticle composite. *Compos Sci Technol* 63: 1599–1605. [https://doi.org/10.1016/S0266-3538\(03\)00061-7](https://doi.org/10.1016/S0266-3538(03)00061-7)
11. Zeng QH, Yu AB, Lu GQ, et al. (2003) Molecular dynamics simulation of organic-inorganic nanocomposites: layering behavior and interlayer structure of organoclays. *Chem Mater* 15: 4732–4738. <https://doi.org/10.1021/cm0342952>
12. Vacatello M (2003) Predicting the molecular arrangements in polymer-based nanocomposites. *Macromol Theor Simul* 12: 86–91. <https://doi.org/10.1002/mats.200390000>
13. Zeng QH, Yu AB, Lu GQ (2005) Interfacial interactions and structure of polyurethane intercalated nanocomposite. *Nanotechnology* 16: 2757–2763. <https://doi.org/10.1088/0957-4484/16/12/002>

14. Allen MP, Tildesley DJ (1989) *Computer Simulation of Liquids*, Oxford: Clarendon Press. <https://doi.org/10.1063/1.2810937>
15. Frenkel D, Smit B (2002) *Understanding Molecular Simulation: from Algorithms to Applications*, 2 Eds., San Diego: Academic Press.
16. Metropolis N, Rosenbluth AW, Marshall N, et al. (1953) Equation of state calculations by fast computing machines. *J Chem Phys* 21: 1087–1092. <https://doi.org/10.1063/1.1699114>
17. Gibson JB, Zhang K, Ke Chen, et al. (1999) Simulation of colloid-polymer systems using dissipative particle dynamics. *Mol Simulat* 23: 1–41. <https://doi.org/10.1080/08927029908022109>
18. Dzwinel V, Yuen DA (2000) A two-level, discrete particle approach for large-scale simulation of colloidal aggregates. *Int J Mod Phys C* 11: 1037–1061. <https://doi.org/10.1142/S0129183100000882>
19. Dzwinel W, Yuen DA (2000) A two-level discrete-particle approach for simulating ordered colloidal structures. *J Colloid Interface Sci* 225: 179–190. <https://doi.org/10.1006/jcis.2000.6751>
20. Chen S, Doolen GD (1998) Lattice Boltzmann method for fluid flows. *Annu Rev Fluid Mech* 30: 329–364. <https://doi.org/10.1146/annurev.fluid.30.1.329>
21. Meyyappan M (2004) *Carbon Nanotubes: Science and Applications*, Boca Raton: CRC Press. <https://doi.org/10.1201/9780203494936>
22. Altevogt P, Ever OA, Fraaije JGEM, et al. (1999) The Meso Dyn project: software for mesoscale chemical engineering. *J Mol Struct* 463: 139–143. [https://doi.org/10.1016/S0166-1280\(98\)00403-5](https://doi.org/10.1016/S0166-1280(98)00403-5)
23. Kawakatsu T, Doi M, Hasegawa A (1999) Dynamic density functional approach to phase separation dynamics of polymer systems. *Int J Mod Phys C* 10: 1531–1540. <https://doi.org/10.1142/S0129183199001315>
24. Morita H, Kawakatsu T, Doi M (2001) Dynamic density functional study on the structure of thin polymer blend films with a free surface. *Macromolecules* 34: 8777–8783. <https://doi.org/10.1021/ma010346+>
25. Computer Simulation of Polymeric Materials (2016) *Computer Simulation of Polymeric Materials: Applications of the OCTA System*, Springer Singapore. <https://doi.org/10.1007/978-981-10-0815-3>
26. Montazeri A, Mehrafrooz B (2018) 14-theoretical modeling of CNT-polymer interactions, In: Rafiee R, *Carbon Nanotube-Reinforced Polymers: From Nanoscale to Macroscale-A Volume in Micro and Nano Technologies*, Elsevier, 347–383. <https://doi.org/10.1016/B978-0-323-48221-9.00014-5>
27. Verma A, Parashar A, Packirisamy M (2018) Atomistic modeling of graphene/hexagonal boron nitride polymer nanocomposites: a review. *WIRES-Comput Mol Sci* 8: e1346. <https://doi.org/10.1002/wcms.1346>
28. Sindu BS, Sasmal S (2015) Evaluation of mechanical characteristics of nano modified epoxy based polymers using molecular dynamics. *Comp Mater Sci* 96: 146–158. <https://doi.org/10.1016/j.commsci.2014.09.003>
29. Hu H, Onyebueke L, Abatan A (2010) Characterizing and modeling mechanical properties of nanocomposites-review and evaluation. *JMMCE* 9: 275–319. <https://doi.org/10.4236/jmmce.2010.94022>
30. Lau KT, Gu C, Hui D (2006) A critical review on nanotube and nanotube/nanoclay related polymer composite materials. *Compos Part B-Eng* 37: 425–436. <https://doi.org/10.1016/j.compositesb.2006.02.020>

31. Sun H (1998) COMPASS: an ab initio force-field optimized for condensed-phase applications overview with details on alkane and benzene compounds. *J Phys Chem B* 102: 7338–7364. <https://doi.org/10.1021/jp980939v>
32. Allinger NL, Yuh YH, Lii JH (1989) Molecular mechanics The MM3 force field for hydrocarbons. *J Am Chem Soc* 111: 8551–8566. <https://doi.org/10.1021/ja00205a001>
33. Lii JH, Allinger NL (1991) The MM3 force field for amides, polypeptides and proteins. *J Comput Chem* 12: 186–199. <https://doi.org/10.1002/jcc.540120208>
34. Allinger NL, Li F, Yan L (1990) Molecular mechanics The MM3 force field for alkenes. *J Comput Chem* 11: 848–867. <https://doi.org/10.1002/jcc.540110708>
35. Allinger NL, Rahman M, Lii JH (1990) A molecular mechanics force field (MM3) for alcohols and ethers. *J Am Chem Soc* 112: 8293–8307. <https://doi.org/10.1021/ja00179a012>
36. Awaja F, Zhang S, Tripathi M, et al. (2016) Cracks, microcracks and fracture in polymer structures: Formation, detection, autonomic repair. *Prog Mater Sci* 83: 536–573. <https://doi.org/10.1016/j.pmatsci.2016.07.007>
37. Zaminpayma E (2014) Molecular dynamics simulation of mechanical properties and interaction energy of polythiophene/polyethylene/poly(p-phenylenevinylene) and CNTs composites. *Polym Compos* 35: 2261–2268. <https://doi.org/10.1002/pc.22891>
38. Arash B, Wang Q, Varadan VK (2014) Mechanical properties of carbon nanotube/polymercomposites. *Sci Rep* 4: 1–8. <https://doi.org/10.1038/srep06479>
39. Arab B, Shokuhfar A (2013) Molecular dynamics simulation of cross-linked epoxy polymers: the effect of force field on the estimation of properties. *J Nano-Electron Phys* 5: 01013.
40. Jeyranpour F, Alahyarizadeh G, Arab B (2015) Comparative investigation of thermal and mechanical properties of cross-linked epoxy polymers with different curing agents by molecular dynamics simulation. *J Mol Graph Model* 62: 157–164. <https://doi.org/10.1016/j.jmngm.2015.09.012>
41. Shenogina NB, Tsige M, Patnaik SS, et al. (2012) Molecular modeling approach to prediction of thermo-mechanical behavior of thermoset polymer networks. *Macromolecules* 45: 5307–5315. <https://doi.org/10.1021/ma3007587>
42. Choi J, Shin H, Yang S, et al. (2015) The influence of nanoparticle size on the mechanical properties of polymer nanocomposites and the associated interphase region: A multiscale approach. *Compos Struct* 119: 365–376. <https://doi.org/10.1016/j.compstruct.2014.09.014>
43. Ingvason GA, Rollin V (2014) Molecular dynamics simulation of a pullout test on a carbon nanotube in a polymer matrix. *MRS OPL* 1700: 61–66. <https://doi.org/10.1557/opl.2014.715>
44. Volodin A, Ahlskog M, Seynaeve E, et al. (2000) Imaging the elastic properties of coiled carbon nanotubes with atomic force microscopy. *Phys Rev Lett* 84: 3342. <https://doi.org/10.1103/PhysRevLett.84.3342>
45. Chen J, Liu B, Gao X, et al. (2018) A review of the interfacial characteristics of polymer nanocomposites containing carbon nanotubes. *RSC Adv* 8: 28048–28085. <https://doi.org/10.1039/C8RA04205E>
46. Mohan R, Fefey E, Kelkar A (2012) Predictive mechanical properties of EPON 862 (DGEBF) cross-linked with curing agent W (DETDA) and SWCNT using MD simulations—Effect of carbon vacancy defects. *53rd AIAA/ASME/ASCE/AHS/ASC Structures, Structural Dynamics and Materials Conference 20th AIAA/ASME/AHS Adaptive Structures Conference 14th AIAA*, 1821, Honolulu, Hawaii. <https://doi.org/10.2514/6.2012-1821>

47. Rahman A, Deshpande P, Radue MS, et al. (2021) A machine learning framework for predicting the shear strength of carbon nanotube-polymer interfaces based on molecular dynamics simulation data. *Compos Sci Technol* 207: 108627. <https://doi.org/10.1016/j.compscitech.2020.108627>
48. Zhang J, Koo B, Subramanian N, et al. (2016) An optimized cross-linked network model to simulate the linear elastic material response of a smart polymer. *J Intel Mat Syst Str* 27: 1461–1475. <https://doi.org/10.1177/1045389X15595292>
49. Park C, Yun GJ (2018) Characterization of interfacial properties of graphene-reinforced polymer nanocomposites by molecular dynamics-shear deformation model. *J Appl Mech* 85: 91007. <https://doi.org/10.1115/1.4040480>
50. Kallivokas SV, Sgouros AP, Theodorou DN (2019) Molecular dynamics simulations of EPON-862/DETDA epoxy networks: structure, topology, elastic constants, and local dynamics. *Soft Matter* 15: 721–733. <https://doi.org/10.1039/C8SM02071J>
51. Aghadavoudi F, Golestanian H, Zarasvand KA (2019) Elastic behavior of hybrid cross-linked epoxy-based nanocomposite reinforced with GNP and CNT: experimental and multiscale modeling. *Polym Bull* 76: 4275–4294. <https://doi.org/10.1007/s00289-018-2602-9>
52. Fasanella N, Sundararaghavan V (2015) Molecular dynamics of SWNT/epoxy nanocomposites. *56th AIAA/ASCE/AHS/ASC Structures, Structural Dynamics and Materials Conference*, Kissimmee, Florida. <https://doi.org/10.2514/6.2015-0124>
53. Kwon W, Han M, Kim J, et al. (2021) Comparative study on toughening effect of PTS and PTK in various epoxy resins. *Polymers* 13: 518. <https://doi.org/10.3390/polym13040518>
54. Al Mahmud H, Radue MS, Chinkanjanarot S, et al. (2019) Multiscale modeling of carbon fiber-graphene nanoplatelet-epoxy hybrid composites using a reactive force field. *Compos Part B-Eng* 172: 628–635. <https://doi.org/10.1016/j.compositesb.2019.05.035>
55. Aboudi J, Arnold SM, Bednarczyk BA (2013) *Micromechanics of Composite Materials*, Elsevier. <https://doi.org/10.1016/C2011-0-05224-9>
56. Pramanik C, Nepal D, Nathanson M, et al. (2018) Molecular engineering of interphases in polymer/carbon nanotube composites to reach the limits of mechanical performance. *Compos Sci Technol* 166: 86–94. <https://doi.org/10.1016/j.compscitech.2018.04.013>
57. Aluko O, Gowtham S, Odegard GM (2020) The assessment of carbon nanotube (CNT) geometry on the mechanical properties of epoxy nanocomposites. *JMMP* 5: 2050005. <https://doi.org/10.1142/S2424913020500058>
58. Yang S (2021) Understanding covalent grafting of nanotubes onto polymer nanocomposites: molecular dynamics simulation study. *Sensors* 21: 2621. <https://doi.org/10.3390/s21082621>
59. Zhu F, Park C, Jin Yun G (2021) An extended Mori-Tanaka micromechanics model for wavy CNT nanocomposites with interface damage. *Mech Adv Mater Struc* 28: 295–307. <https://doi.org/10.1080/15376494.2018.1562135>
60. Subramanian N, Rai A, Chattopadhyay A (2017) Atomistically derived cohesive behavior of interphases in carbon fiber reinforced CNT nanocomposites. *Carbon* 117: 55–64. <https://doi.org/10.1016/j.carbon.2017.02.068>
61. Bamane SS, Gaikwad PS, Radue MS, et al. (2021) Wetting simulations of high-performance polymer resins on carbon surfaces as a function of temperature using molecular dynamics. *Polymers* 13: 2162. <https://doi.org/10.3390/polym13132162>
62. Bandyopadhyay A, Valavala PK, Clancy TC, et al. (2011) Molecular modeling of crosslinked epoxy polymers: The effect of crosslink density on thermomechanical properties. *Polymer* 52: 2445–2452. <https://doi.org/10.1016/j.polymer.2011.03.052>

63. Bandyopadhyay A, Odegard GM (2013) Molecular modeling of physical aging in epoxy polymers. *J Appl Polym Sci* 128: 660–666. <https://doi.org/10.1002/app.38245>
64. Wang Z, Yang X, Wang Q, et al. (2011) Epoxy resin nanocomposites reinforced with ionized liquid stabilized carbon nanotubes. *Int J Smart Nano Mat* 2: 176–193. <https://doi.org/10.1080/19475411.2011.594104>
65. Hadipeykani M, Aghadavoudi F, Toghraie D (2020) A molecular dynamics simulation of the glass transition temperature and volumetric thermal expansion coefficient of thermoset polymer based epoxy nanocomposite reinforced by CNT: a statistical study. *Physica A* 546: 128384. <https://doi.org/10.1016/j.physa.2019.123995>
66. Henry MM, Thomas S, Alberts MT, et al. (2020) General-purpose coarse-grained toughened thermoset model for 44DDS/DGEBA/PES. *Polymers* 12: 2547. <https://doi.org/10.3390/polym12112547>
67. Crawford AO, Hamerton I, Cavalli G, et al. (2012) Quantifying the effect of polymer blending through molecular modelling of cyanurate polymers. *PLoS ONE* 7: e44487. <https://doi.org/10.1371/journal.pone.0044487>
68. Hall SA, Howlin BJ, Hamerton I, et al. (2012) Solving the problem of building models of crosslinked polymers: An example focussing on validation of the properties of crosslinked epoxy resins. *PLoS ONE* 7: e42928. <https://doi.org/10.1371/journal.pone.0042928>
69. Koo B, Liu Y, Zou J, et al. (2014) Study of glass transition temperature (T<sub>g</sub>) of novel stress-sensitive composites using molecular dynamic simulation. *Model Simul Mater Sc* 22: 5018. <https://doi.org/10.1088/0965-0393/22/6/065018>
70. Sul JH, Prusty BG, Kelly DW (2014) Application of molecular dynamics to evaluate the design performance of low aspect ratio carbon nanotubes in fibre reinforced polymer resin. *Compos Part A-Appl S* 65: 64–72. <https://doi.org/10.1016/j.compositesa.2014.03.004>
71. Farhadinia M, Arab B, Jam J (2016) Mechanical properties of CNT-reinforced polymer nano-composites: A molecular dynamics study. *MACS* 3: 113–121. <https://doi.org/10.22075/mac.2016.473>
72. Emmanwori L, Shinde DK, Kelkar AD (2013) Mechanical properties assesment of electrospun TEOS nanofibers with EPON 862/W resin system in a fiber glass composite. *SAMPE Technical Conference Proceedings*, Wichita, KS, 21–24. Available from: <https://www.nasampe.org/store/viewproduct.aspx?ID=4403730>.
73. Wang, YT, Wang CS, Yin YH, et al. (2012) Carboxyl-terminated butadiene-acrylonitrile-toughened epoxy/carboxyl-modified carbon nanotube nanocomposites: Thermal and mechanical properties. *Express Polym Lett* 6: 719–728. <https://doi.org/10.3144/expresspolymlett.2012.77>
74. Shinde DK, Kelkar AD (2014) Effect of TEOS electrospun nanofiber modified resin on interlaminar shear strength of glass fiber/epoxy composite. *WASET Org* 8: 54–60.
75. Al Hasan NHJ (2018) Prediction of mechanical properties of EPON 862 (DGEBF) cross-linked with curing agent (TETA) and SiO<sub>2</sub> nanoparticle based on materials studio. *IOP Conf Ser-Mater Sci Eng* 454: 012139. <https://doi.org/10.1088/1757-899X/454/1/012139>
76. Estridge CE (2018) The effects of competitive primary and secondary amine reactivity on the structural evolution and properties of an epoxy thermoset resin during cure: A molecular dynamics study. *Polymer* 141: 12–20. <https://doi.org/10.1016/j.polymer.2018.02.062>
77. Giannopoulos GI, Georgantzinis SK (2021) Thermomechanical behavior of bone-shaped SWCNT/polyethylene nanocomposites via molecular dynamics. *Materials* 14: 2192. <https://doi.org/10.3390/ma14092192>

78. Agarwal BD, Broutman LJ (1974) Three-dimensional finite element analysis of spherical particle composites. *Fibre Sci Technol* 7: 63–77. [https://doi.org/10.1016/0015-0568\(74\)90006-2](https://doi.org/10.1016/0015-0568(74)90006-2)
79. Treacy MJ, Ebbesen TW, Gibson JM (1996) Exceptionally high Young's modulus observed for individual carbon nanotubes. *Nature* 381: 678–680. <https://doi.org/10.1038/381678a0>
80. Popov VN, Van Doren VE, Balkanski M (2020) Elastic properties of single-walled carbon nanotubes. *Phys Rev B* 61: 3078–3084. <https://doi.org/10.1103/PhysRevB.61.3078>
81. Li C, Chou T (2006) Multiscale modeling of compressive behavior of carbon nanotube/polymer composites. *Compos Sci Technol* 66: 2409–2414. <https://doi.org/10.1016/j.compscitech.2006.01.013>
82. Shi D, Feng X, Jiang H, et al. (2005) Multiscale analysis of fracture of carbon nanotubes embedded. *Int J Fract* 134: 369–386. <https://doi.org/10.1007/s10704-005-3073-1>
83. Bagha AK, Bahl S (2020) Finite element analysis of VGCF/pp reinforced square representative volume element to predict its mechanical properties for different loadings. *Mater Today Proc* 39: 54–59. <https://doi.org/10.1016/j.matpr.2020.06.108>
84. Tserpes KI, Papanikos P, Labeas G, et al. (2007) Multi-scale modeling of tensile behavior of carbon nanotube-reinforced composites. *Theor Appl Fract Mech* 49: 51–60. <https://doi.org/10.1016/j.tafmec.2007.10.004>
85. Sanei SHR, Doles R (2020) Representative volume element for mechanical properties of carbon nanotube nanocomposites using stochastic finite element analysis. *J Eng Mater Technol* 142: 031004. <https://doi.org/10.1115/1.4045708>
86. Tserpes KI, Papanikos P (2006) A progressive fracture model for carbon nanotubes. *Compos Part B-Eng* 37: 662–669. <https://doi.org/10.1016/j.compositesb.2006.02.024>
87. Tserpes KI, Papanikos P, Labeas G, et al. (2008) Multi-scale modeling of tensile behavior of carbon nanotube-reinforced composites. *Theoret Appl Fract Mech* 49: 51–60. <https://doi.org/10.1016/j.tafmec.2007.10.004>
88. Bhuiyan MA, Pucha RV, Worthy J, et al. (2013) Understanding the effect of CNT characteristics on the tensile modulus of CNT reinforced polypropylene using finite element analysis. *Comp Mater Sci* 79: 368–376. <https://doi.org/10.1016/j.commat.2013.06.046>
89. Chawla N, Sidhu RS, Ganesh VV (2006) Three-dimensional visualization and microstructure-based modeling of deformation in particle-reinforced composites. *Acta Mater* 54: 1541–1548. <https://doi.org/10.1016/j.actamat.2005.11.027>
90. Georgantzinou SK, Antoniou PA, Giannopoulos GI, et al. (2021) Design of laminated composite plates with carbon nanotube inclusions against buckling: Waviness and agglomeration effects. *Nanomaterials* 11: 2261. <https://doi.org/10.3390/nano11092261>
91. Georgios I. Giannopoulos, Ilias G. Kallivokas (2014), Mechanical properties of graphene based nanocomposites incorporating a hybrid interphase. *Finite Elem Anal Des* 90: 31–40. <https://doi.org/10.1016/j.finel.2014.06.008>.



AIMS Press

© 2023 the Author(s), licensee AIMS Press. This is an open access article distributed under the terms of the Creative Commons Attribution License (<http://creativecommons.org/licenses/by/4.0>)